

Design and identification of a novel, functionally subtype selective GABA positive allosteric modulator (PF-06372865).

Robert M. Owen, David C Blakemore, Lishuang Cao, Neil Flanagan, Rebecca Fish, Karl R Gibson, Rachel Gurrell, Chan Woo Huh, Juha Kammonen, Elisabeth Mortimer-Cassen, Sarah Nickolls, Kiyoyuki Omoto, Dafydd R Owen, Andrew Pike, David C. Pryde, David Reynolds, Rosemarie Roeloffs, Colin R. Rose, Clara Stead, Mifune Takeuchi, Joseph S Warmus, and Christine Watson

J. Med. Chem., **Just Accepted Manuscript** • DOI: 10.1021/acs.jmedchem.9b00322 • Publication Date (Web): 09 Apr 2019

Downloaded from <http://pubs.acs.org> on April 10, 2019

Just Accepted

“Just Accepted” manuscripts have been peer-reviewed and accepted for publication. They are posted online prior to technical editing, formatting for publication and author proofing. The American Chemical Society provides “Just Accepted” as a service to the research community to expedite the dissemination of scientific material as soon as possible after acceptance. “Just Accepted” manuscripts appear in full in PDF format accompanied by an HTML abstract. “Just Accepted” manuscripts have been fully peer reviewed, but should not be considered the official version of record. They are citable by the Digital Object Identifier (DOI®). “Just Accepted” is an optional service offered to authors. Therefore, the “Just Accepted” Web site may not include all articles that will be published in the journal. After a manuscript is technically edited and formatted, it will be removed from the “Just Accepted” Web site and published as an ASAP article. Note that technical editing may introduce minor changes to the manuscript text and/or graphics which could affect content, and all legal disclaimers and ethical guidelines that apply to the journal pertain. ACS cannot be held responsible for errors or consequences arising from the use of information contained in these “Just Accepted” manuscripts.



Design and identification of a novel, functionally subtype selective GABA_A positive allosteric modulator (PF-06372865).

Robert M. Owen,^{b} David Blakemore,^b Lishuang Cao,^c Neil Flanagan,^e Rebecca Fish,^c Karl R. Gibson,^f Rachel Gurrell,^c Chan Woo Huh,^g Juha Kammonen,^c Elisabeth Mortimer-Cassen,^d Sarah Nickolls,^c Kiyoyuki Omoto,^b Dafydd Owen,^g Andy Pike,^a David C. Pryde,^b David S. Reynolds,^c Rosemarie Roeloffs,^h Colin Rose,^g Clara Stead,^c Mifune Takeuchi,^f Joseph S. Warmus,^g Christine Watson^f*

^aPharmacokinetics, Dynamics and Metabolism, ^bWorldwide Medicinal Chemistry, ^cPfizer Neusentis, ^dGlobal Safety Group,

^ePharmaceutical Sciences, Pfizer Ltd., The Portway, Granta Park, Cambridge, CB21 6GS; ^fWorldwide Medicinal Chemistry Sandwich Laboratories, Ramsgate Road, Sandwich, Kent CT13 9NJ, United Kingdom; ^gWorldwide Medicinal Chemistry, Pfizer Global Research & Development, 558 Eastern Point Road, Groton, Connecticut 06340, United States; ^hPfizer Icagen, Research Triangle Park, North Carolina 27703, United States

KEYWORDS: GABA_A, selective positive allosteric modulator, PAM, ion channel, CNS, clinical

ABSTRACT: The design, optimization and evaluation of a series of novel imidazopyridazine-based subtype-selective positive allosteric modulators (PAMs) for the GABA_A ligand-gated ion channel are described. From a set of initial hits multiple subseries were designed and evaluated based on binding affinity and functional activity. As designing in the desired level of functional selectivity proved difficult, a probability-based assessment was performed to focus the project's efforts on a single subseries which had the greatest odds of delivering the target profile. These efforts ultimately led to the identification of two pre-candidates from this subseries, which were advanced to pre-clinical safety studies and subsequently to the identification of the clinical candidate PF-06372865.

INTRODUCTION

Neuronal signaling via the γ -amino butyric acid (GABA)-type A (GABA_A) receptor plays a critical role in a wide range of processes within the central nervous system (CNS). The GABA_A receptor belongs to the Cys-loop family of ligand gated ion channels and modulates the flow of chloride anions across the synaptic junction upon binding of its endogenous ligand GABA.¹ The receptor is comprised of five subunits, of which sixteen

different subtypes have been identified ($\alpha 1-6$, $\beta 1-3$, $\gamma 1-3$, δ , ϵ , θ and π). However, relatively few combinations have been shown to exist in the CNS with the overwhelming majority of receptors consisting of two α , two β and one γ subunit, although other subunit compositions, such as $2\alpha 2\beta\delta$ have also been identified.²⁻⁴ GABA is the major inhibitory neurotransmitter in the CNS and drugs targeting the GABA_A receptor show diverse pharmacology, including anxiolytic, hypnotic and anti-convulsant effects, as well as the receptor being involved in the processes of cognition and the perception of pain.⁵⁻⁷ There are several different classes of marketed GABAergic drugs, and modulation of the function of the GABA_A receptor via small molecules has remained an active area of research since the initial discovery and clinical success of the 1,4-benzodiazapine class of therapeutics in the 1960s.⁸

Classical benzodiazepines act as non-selective positive allosteric modulators (PAMs) of the action of GABA on $\alpha 1$ -, $\alpha 2$ -, $\alpha 3$ - and $\alpha 5$ -subunit-containing receptors where present with a $\gamma 2$ subunit. While they are highly effective drugs, with both anxiolytic and anti-convulsant properties, they also exhibit undesirable properties including sedation, cognitive deficits, potential for abuse and dependence, and significant potentiation of these effects by alcohol.

1
2
3 However, it has been demonstrated, using a combination of
4 studies in genetically modified mice and using compounds showing
5 subtype-selective modulation, that different aspects of
6 benzodiazepine pharmacology can be attributed to different α
7 subunits. For example, signaling via $\alpha 1$ -containing receptors
8 contributes significantly to the sedative effects of 1,4-
9 benzodiazepines.⁹ In contrast, the $\alpha 2$ - and $\alpha 3$ -containing
10 receptors have stronger links to anxiety related activities,¹⁰⁻¹²
11 while some of the effects on cognitive function are tied to $\alpha 5$ -
12 containing receptors.¹³ In addition, $\alpha 1$ - and $\alpha 2$ -containing
13 receptors have been linked to the anticonvulsant activity of
14 benzodiazepines.^{10, 14} Finally, modulation of $\alpha 2$ - and $\alpha 3$ -
15 containing GABA_A receptors in the spinal cord, results in pain
16 relief in preclinical studies.¹⁰ Therefore, subunit selective-
17 allosteric modulators have the potential to retain the
18 therapeutic benefits of classical benzodiazepines while
19 minimizing the associated side effects.^{8-9, 15}

20
21 With these ideas in mind, various research groups have explored
22 the development of $\alpha 1$ -sparing, $\alpha 2/3$ PAMs for the treatment of
23 anxiety and other disorders.^{8-9, 16} During the course of these
24 studies it proved difficult to identify compounds that exhibited
25 the desired selectivity profile by selectively binding to the $\alpha 2$
26 or $\alpha 3$ -subunit-containing receptors over those containing $\alpha 1$
27 subunits. This is presumably due to conservation of key-binding

residues in the benzodiazepine binding site which is located at the α/γ interface of the GABA_A receptor complex¹⁷⁻¹⁸. Instead, the researchers found that selectivity could be more readily obtained functionally, i.e. a given compound binds to different receptor subunit combination with comparable affinity but promotes very different levels of functional activity. Ultimately this approach proved successful and has led to the identification of a broad range of both clinical and preclinical compounds (*vide infra*). However, to date, no new approved drugs have resulted from this work.

Herein we describe our efforts towards the identification of a novel $\alpha 1$ -sparing GABA_A PAM. From initial file screening leads, we successfully optimized the imidazopyridazine series to ultimately yield two compounds with preclinical profiles that were suitable for advancement to pre-clinical safety studies. From these safety studies, compound PF-06372865 was selected for advancement into clinical studies to explore the benefits of subtype selective GABA_A PAMs in humans.^{8-9, 16}

TARGET COMPOUND PROFILE

Beyond the standard desired preclinical profile for a safe and developable CNS-penetrant agent,¹⁹⁻²¹ our initial goal was to establish the required levels of functional selectivity for $\alpha 2$ over $\alpha 1$ as measured in our assays in order to ensure that any potential candidate would exhibit the desired pharmacology

profile in the clinic. As mentioned previously, multiple functionally selective GABA_A PAMs have been advanced into clinical trials. Of these, clinical data has been disclosed for three key compounds, MRK-409, TPA-023 and TPA-023B (Figure 1)^{8, 22-26}. MRK-409, which exhibits selectivity for $\alpha 2$ over $\alpha 1$ in functional assays but still shows moderate $\alpha 1$ activity, was markedly sedative in man even though this was not predicted from preclinical species.²⁷ In contrast, TPA-023 and TPA-023B, which both show selectivity as well as decreased efficacy at $\alpha 1$ relative to MRK-409, were both well tolerated and demonstrated reduced sedative effects in human clinical trials.²⁸⁻³⁰ TPA-023 also showed preliminary evidence of efficacy in both anxiety and schizophrenia in man.³⁰ Based on this analysis, we set a maximal $\alpha 1$ enhancement of the GABA response in our in vitro systems of around 20% and a minimum $\alpha 2$ enhancement of 50% as our target PAM profile for any potential candidates. We also wanted to avoid significant negative allosteric modulation of $\alpha 1$ -containing receptors, as this had been demonstrated to cause seizures in preclinical studies. Subsequent to the initiation of our internal studies, two additional functionally selective GABA_A PAMs (AZD7325³¹ and NS11821³²) have been reported in the literature.

Structure	Name	$\alpha 2$ Ki \pm SEM	$\alpha 1$ PAM \pm SEM (%) ^a	$\alpha 2$ PAM \pm SEM (%) ^b
-----------	------	-------------------------	-------------------------------------------	-------------------------------------------

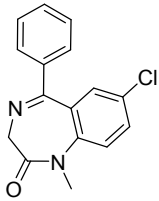
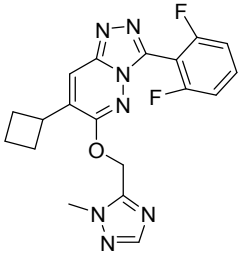
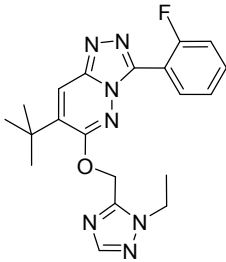
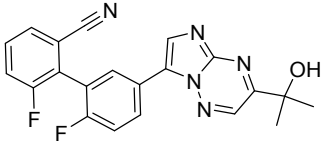
		(nM)		
	Diazepam	48.3 ± 27.4 (n=8)	216 ± 3 (n=422)	293 ± 4 (n=410)
	MRK-409	0.81 ± 0.4 (n=10)	56 ± 5 (n=26)	80 ± 3 (n=31)
	TPA-023	0.54 ± 0.2 (n=31)	21 ± 1 (n=56)	41 ± 2 (n=59)
	TPA-023B	2.14 ± 0.7 (n=37)	19 ± 1 (n=273)	81 ± 1 (n=315)

Table 1. GABA_A PAMs for which clinical data has been reported. α₂ K_i and functional activity values were measured as described here.^{33–35} Percentage values refer to the level of enhancement measured after activation of the receptor with GABA as described here.^{33–35} a,b GABA_A functional activity were measured at 100-times the compound's K_i.

IDENTIFICATION AND INITIAL OPTIMIZATION OF IMIDAZOPYRIDAZINE SERIES

Based on historical literature precedent and our own internal experience, although SAR for functional selectivity exists within a given chemotype, generally it is quite "spiky" with minor changes in structure leading to very different functional profiles. As a result, early in the lifetime of the program we adopted a strategy of profiling multiple series in parallel to maximize our chances of identifying a potent, functionally selective molecule that could be developed as a once daily agent.

As a starting point for our design efforts, the project team applied a range of ligand-based techniques based on structures from the literature that functioned as GABA PAMs to find starting points from within our internal compound collection. These methods included similarity-based searches as well as molecular overlays to determine key pharmacophoric elements which, allowed us to ultimately arrive at the following three series (Figure 1). As a general design strategy, we explored a range of different heterocyclic cores decorated with substituents as indicated including directly linked aromatic or heterocyclic groups, alkyl groups and heteroatom (e.g. O, N) linked substituents. Each of these series was progressed in parallel and evaluated on their ability to deliver affinity, functional activity and an appropriate in vitro ADME profile. For the purpose of this discussion we will focus on the

optimization of one of these series, the imidazopyridazines, series 2, but will revisit the overall merits of each series in terms of providing the required affinity, ADME and functional profiles.

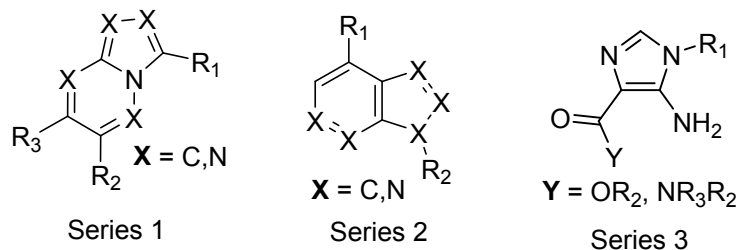
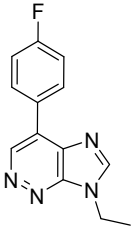
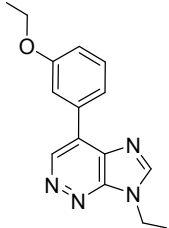
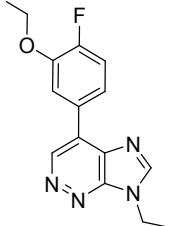
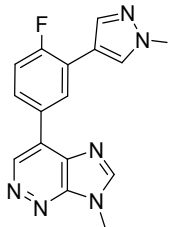


Figure 1. Markush structures for the series 1-3.

Table 2 outlines some of the initial hits within this series, which were identified via a mixture of ligand-based methods. Compound **1** and **2** suggested that reasonable affinity for the GABA_A receptor could be obtained via an imidazopyridazine core substituted by a simple aryl group and that alkyl ether groups were tolerated on this aryl ring system. A para-fluoro group could provide a modest improvement in affinity over the equivalent des-fluoro scaffold (Compound **2** vs **3**). Optimization of these initial leads rapidly demonstrated that the overall affinity of this scaffold could be improved via introduction of either a second direct-linked or ether-linked aromatic group (Compound **4-6**). Although neither compound **4** or **5** exhibited a promising functional profile, compound **6** exhibited the desired

level of functional selectivity as well as an in vitro profile consistent with good CNS-penetration, which suggested that further work within this scaffold was warranted.

Structure	ID	$\alpha 2$ Ki \pm SEM (nM)	Lip E ^a	$\alpha 1$ PAM \pm SEM (%) ^b	$\alpha 2$ PAM \pm SEM (%) ^c	LogD ^d	HLM ^e Clint (μ L/min/mg)	MDR ^f
	1	274.6 \pm 57.4 (n=2)	4.3	ND	ND	2.3	105	ND
	2	367.3 \pm 114.4 (n=2)	4.0	ND	ND	2.5	ND	ND
	3	119.5 \pm 20.3 (n=2)	4.5	ND	ND	2.5	ND	ND
	4	10 \pm 7.4 (n=2)	5.8	-55 \pm 2 (n=4)	-4 \pm 3 (n=6)	2.3	47	ND

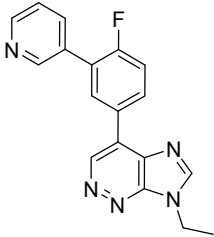
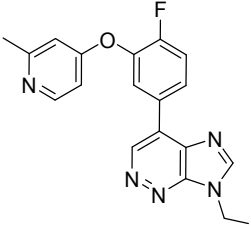
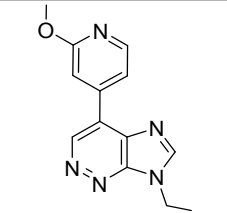
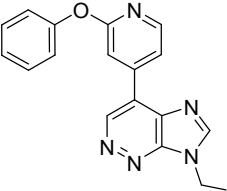
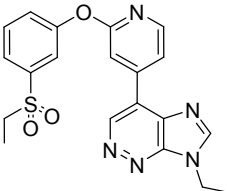
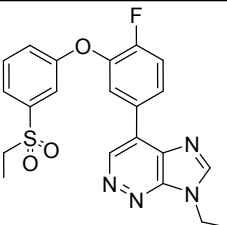
	5	28.9 ± 6.6 (n=5)	4.9	-48 ± 10 (n=2)	10 ± 1 (n=4)	2.6	78	1.0
	6	33.3 ± 15.1 (n=3)	4.8	-22 ± 4 (n=4)	54 ± 5 (n=7)	2.6	65	2.7

Table 2. Initial hits within the imidazopyridazine series. α_2 Ki and α_1/α_2 PAM values were measured as described here.³³⁻³⁵ ^aLogD are measured values or if calculated (internal logD model) are in italics. ^{b,c}GABA_A functional activity were measured at 100-times the compound's K_i. ^dLipE values are calculated (pK_i - logD) from measured logD values when possible or from calculated logD. ^eHLM Clint (μL/min/mg), in vitro human microsomal stability measurement. ^fMDR er: Ratio from the MS-based quantification of apical/basal and basal/apical transfer rates of test compound at 2 μM across confluent monolayers of MDR1-transfected MDCK cells.

Based on the results obtained for Compound **6**, we sought to further optimize this aryl-ether linked subseries towards a potential candidate. In order to synthesize a broad range of compounds within this subseries, we initially examined whether the more synthetically-accessible pyridyl linked ethers would provide the desired activity profile. Compound **7**, while weaker

than our other starting points, was still quite efficient and changing from a methoxy to phenyl ether provided a significant boost in affinity with equal efficiency (LipE) but without the desired functional profile. Unfortunately, attempts to further optimize the profile of any pyridyl-based ethers met with limited success and when compared with the fluoro-phenyl group (Compound **9** vs **10**) the pyridyl moiety did not bring any advantages and was not explored any further. Additional linkers attached to the ether moiety were also explored (Compound **11** and **12**) and provided good affinity and efficiency but did not yield the required functional profile. Examining the profile of compound **10**, we then explored other polar aromatic groups with the hope of improving efficiency, the functional selectivity profile as well as overall metabolic stability. Changing from the phenyl sulfone (**10**) to a pyrimidyl nitrile (Compound **13**) provided a small improvement in efficiency and stability and more importantly a marked improvement in the functional selectivity profile. Further optimization yielded Compound **14** which again had the desired functional profile but lacked the desired level of metabolic stability for further progression. Based on metabolite identification work for related compounds, we hypothesized that compound **14** was being N-dealkylated at the imidazo ring system which may contribute to its high turnover in human microsomes. Conversion of the ethyl group to either a

cyclopropyl (**15**) or isopropyl (**16**) led to compounds with an improvement in overall stability while maintaining the functional selectivity. However, in both cases, the compounds lost affinity and efficiency and could not be progressed further.

Structure	ID	$\alpha 2$ Ki \pm SEM (nM)	Lip E ^a	$\alpha 1$ PAM \pm SEM (%) ^b	$\alpha 2$ PAM \pm SEM (%) ^c	LogD ^d	HLM ^e Clint (μ L/min/mg)	MDR ^f
	7	961.6 \pm 23.4 (n=2)	4.6	ND	ND	1.5	ND	ND
	8	61.2 \pm 11 (n=4)	4.6	-24 \pm 1 (n=5)	13 \pm 3 (n=5)	2.6	51	1.2
	9	1141.9 \pm 160.8 (n=3)	4.2	ND	ND	1.6	<8	2.0
	10	77.3 \pm 19.1 (n=2)	4.8	14 \pm 3 (n=9)	37 \pm 4 (n=5)	2.3	127	2.8

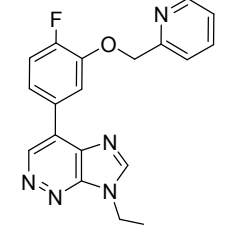
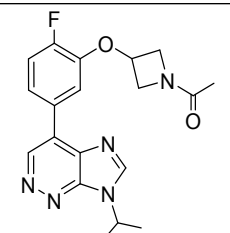
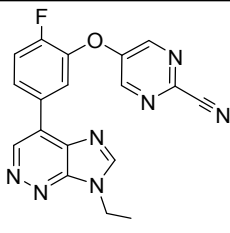
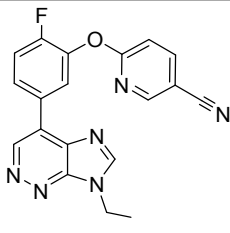
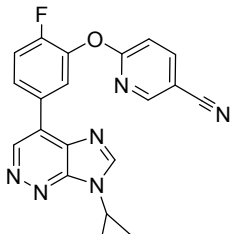
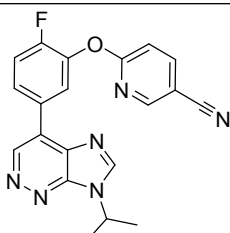
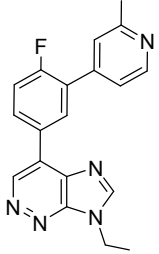
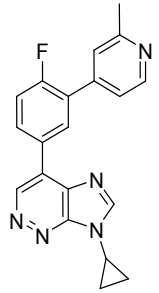
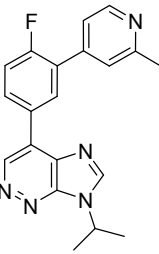
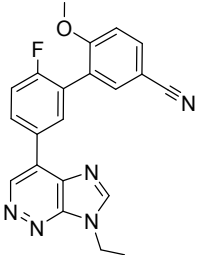
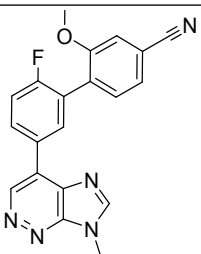
	11	22.8 ± 2.6 (n=2)	5.2	7 ± 4 (n=8)	10 ± 2 (n=19)	2.5	41	4.8
	12	33.3 ± 3.9 (n=2)	5.8	-6 ± 4 (n=6)	6 ± 5 (n=6)	1.6	<8	3.4
	13	81.4 ± 97.3 (n=4)	5.1	13 ± 2 (n=6)	87 ± 5 (n=9)	2.0	49	0.8
	14	30.6 ± 5.7 (n=2)	5.2	-3 ± 3 (n=15)	96 ± 5 (n=19)	2.3	65	1.4
	15	219.1 ± 28.1 (n=2)	4.3	10 ± 2 (n=4)	78 ± 14 (n=6)	2.3	17	1.1
	16	358.3 ± 225 (n=2)	3.7	3 ± 4 (n=3)	89 ± 10 (n=4)	2.7	38	1.1

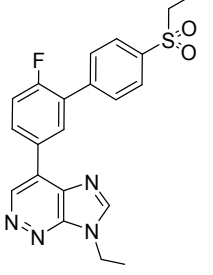
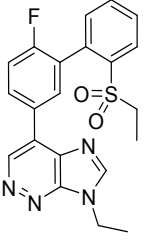
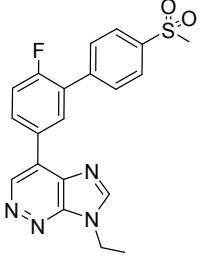
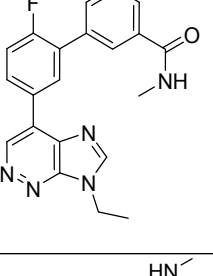
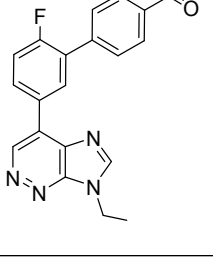
Table 3. Ether-based imidazopyridazine subseries. α_2 Ki and α_1/α_2 PAM values were measured as described here.³³⁻³⁵ a LogD are

measured values or if calculated (internal logD model) are in italics. ^{b,c}GABA_A functional activity were measured at 100-times the compound's K_i. ^dLipE values are calculated (pK_i - logD) from measured logD values when possible or from calculated logD. ^eHLM Clint (μL/min/mg), in vitro human microsomal stability measurement. ^fMDR er: Efflux ratio from the MS-based quantification of apical/basal and basal/apical transfer rates of test compound at 2 μM across confluent monolayers from MDR1-transfected MDCK cells.

In parallel to the optimization efforts described above, we also sought to optimize the profile of compound **5**, looking for modifications that could improve the overall functional profile of the compounds. Changing the pyridine isomer led to compound **17** which immediately showed an improvement in efficiency and met our target profile for functional selectivity. As before in the ethers, this compound was too unstable to progress and attempts to mitigate that problem through altering the imidazole substituent were unsuccessful (Compound **18** and **19**). Interestingly, the three different substituents did not have a profound effect on the affinity of the compounds unlike the ether-linked compounds. However, the isopropyl substituent did lead to an increase in α1 functional activity relative to the α2 activity. As a result of these two observations, the N-ethyl

imidazole became the preferred substituent in subsequent rounds of optimization. Moving away from the pyridyl ring demonstrated that phenyl rings containing polar groups could provide good affinity along with excellent functional selectivity (Compound **20**). However, while a subtle change in the arrangement of those polar groups maintained affinity (Compound **21**), they also led to a large decrease in functional activity. Other polar groups were well tolerated in terms of the affinity of these directly linked aryl groups (Compounds **22** - **27**) and also led to compounds that were both stable and CNS penetrant. However, as before, small changes in structure could lead to moderate to large changes in function. For example, presentation of either a sulfone or amide moiety in the para position of the aryl ring (Compound **22** and Compound **26**) was the most optimal in terms of binding affinity. In the case of compound **22**, while this compound showed the desired functional selectivity, truncation of the ethyl sulfone to the methyl sulfone decreased both $\alpha 1$ and $\alpha 2$ activity below our desired threshold. In addition, the methyl amide (**26**) appeared to be a good bioisostere for the ethyl sulfone in terms of binding affinity, but this compound lost its functional selectivity. One final interesting SAR observation is the effect of ortho substituents on binding affinity with the ortho-fluoro group (**27**) providing an improvement in affinity and efficiency.

Structure	ID	$\alpha 2$ Ki \pm SEM (nM)	Lip E ^a	$\alpha 1$ PAM \pm SEM (%) ^b	$\alpha 2$ PAM \pm SEM (%) ^c	LogD ^d	HLM ^e Clint (μ L/min/mg)	MDR ^f
	17	13.4 \pm 5.8 (n=2)	5.0	-5 \pm 8 (n=3)	71 \pm 3 (n=11)	2.9	157	1.1
	18	20.3 \pm 4.8 (n=25)	4.8	-6 \pm 4 (n=8)	68 \pm 5 (n=10)	2.9	42	1.2
	19	34.0 \pm 16 (n=2)	4.4	57 \pm 10 (n=2)	103 \pm 12 (n=3)	3.1	102	ND
	20	23.6 \pm 0.8 (n=2)	4.6	-4 \pm 6 (n=8)	181 \pm 9 (n=7)	3.1	66	ND
	21	8.8 \pm 2.2 (n=2)	4.9	-40 \pm 2 (n=6)	31 \pm 2 (n=6)	3.2	32	1.4

	22	21.7 ± 2.4 (n=31)	4.8	-13 ± 1 (n=32)	85 ± 3 (n=36)	2.9	<13	1.9
	23	373.1 ± 21.3 (n=2)	4.0	ND	ND	2.4	9	ND
	24	17.7 ± 5.9 (n=3)	5.2	-15 ± 7 (n=3)	33 ± 5 (n=8)	2.5	10	2.2
	25	23.2 ± 9.5 (n=2)	4.8	-10 ± 7 (n=3)	30 ± 4 (n=9)	2.8	40	2.4
	26	6.7 ± 3.7 (n=3)	5.3	-41 ± 4 (n=4)	21 ± 2 (n=28)	2.9	16	3.4

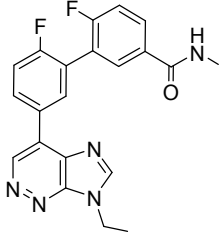
	27	6.8 ± 3.7 (n=4)	5.1	-11 ± 4 (n=9)	17 ± 5 (n=12)	3.0	34	5.2
-----------------------------------------------------------------------------------	-----------	--------------------	-----	------------------	------------------	-----	----	-----

Table 4. Direct linked aryl-based imidazopyridazine subseries.

α_2 Ki and α_1/α_2 PAM values were measured as described here.³³⁻³⁵

^aLogD are measured values or if calculated (internal logD model) are in italics. ^{b,c}GABA_A functional activity were measured at 100-times the compound's K_i. ^dLipE values are calculated (pK_i - logD) from measured logD values when possible or from calculated logD. ^eHLM Clint (μL/min/mg), in vitro human microsomal stability measurement. ^fMDR er: Ratio from the MS-based quantification of apical/basal and basal/apical transfer rates of test compound at 2 μM across contiguous monolayers from MDR1-transfected MDCK cells.

PROBABILITY ASSESSMENT OF ACTIVE SERIES

Although good progress had been made with the various rounds of optimization described above for the imidazopyridazine series, at this stage in the project we did not feel we had identified a compound that was of sufficient quality to nominate as a development candidate. In addition to the work undertaken on the imidazopyridazine series, the project team also worked to optimize two orthogonal series to provide alternative chemotypes with similar selectivity and affinity profiles. Given the spiky

SAR observed across all three series for functional activity, in order to focus our efforts on the series with the best chance of delivering a candidate, we analyzed the probability that each series could deliver in terms of affinity, HLM and CNS-penetration (as measured by MDR efflux ratios) and functional selectivity (Figure 2, Imidazopyridazine series = Series 2).

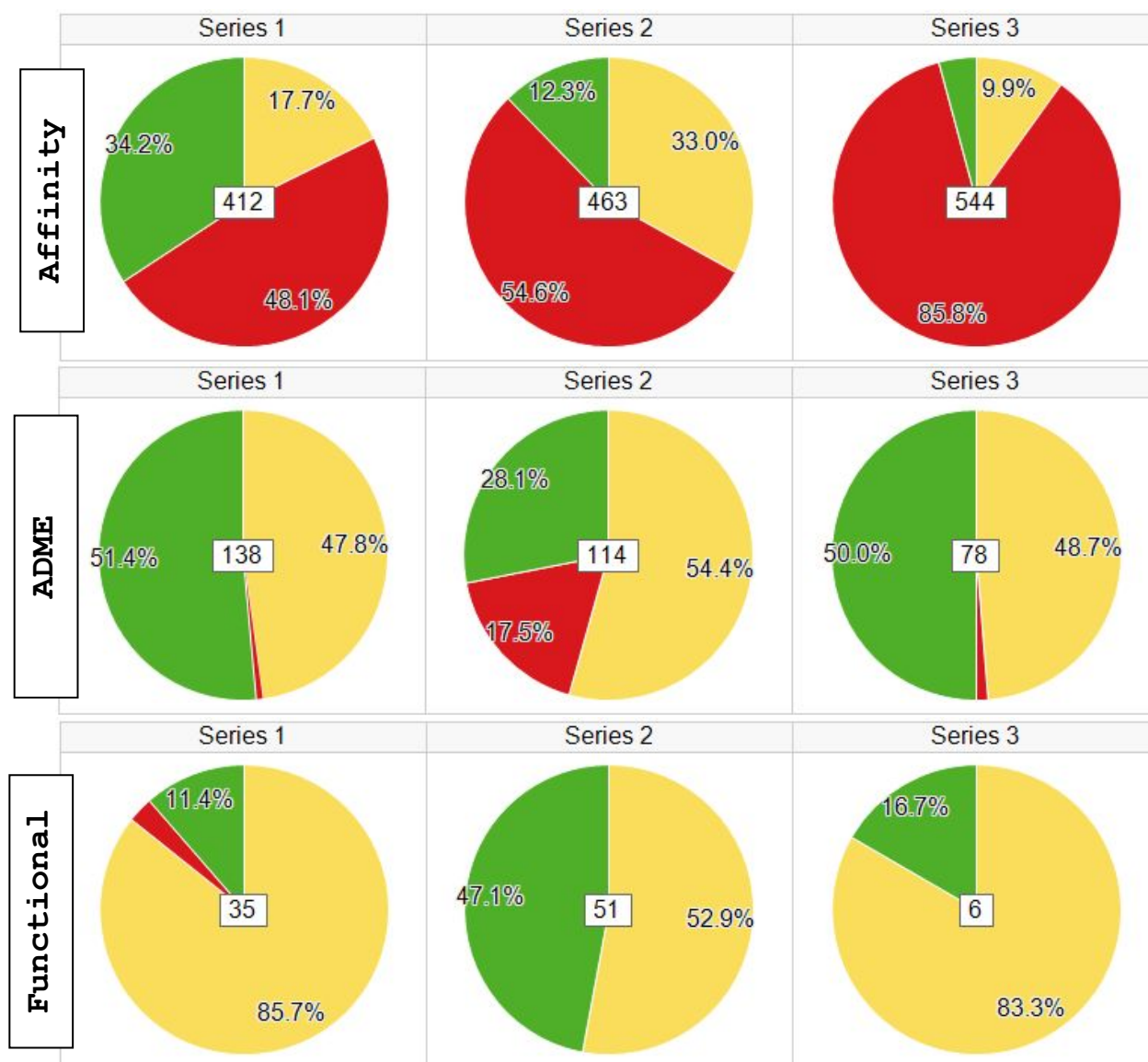


Figure 2. Probability analysis of the project's three main series (Series 2 is the imidazopyradine series) on the basis of:

Affinity: $\alpha_2 K_i < 10$ nM Green, > 40 nM Red. ADME: **HLM** < 20 AND MDR $er < 2.5$ Green, **HLM** > 40 AND MDR $er > 4.0$ Red. **Functional:** α_1 PCT < 20 and α_2 PCT > 50 Green, α_1 PCT > 50 AND $\alpha_2 < 40$ Red. The total number of compounds contained in each pie chart is shown at the chart's center.

Based on this analysis, despite reasonable ADME properties Series 3 was clearly compromised by the low likelihood of achieving adequate affinity. Based on affinity and ADME the choice between Series 1 and 2 was less clear, however, Series 2 clearly had the best chance of obtaining the desired level of functional selectivity. This analysis was extended to the two main subseries within Series 2 (Figure 3), the direct linked and ether linked scaffolds discussed above and clearly showed that the direct linked subseries was far more likely to yield the desired functional profile. For both analyses, none of the probabilities quoted for the three parameters indicate that any series was any more likely than the others for finding a single molecule that combined all three of these features. However, we believed that problems like affinity and ADME would be much more soluble and less "spiky" in terms of SAR than maintaining functional selectivity within a series and therefore shifted all

our design efforts to identifying a suitable candidate from the direct-linked imidazopyridazine series (Series 2).

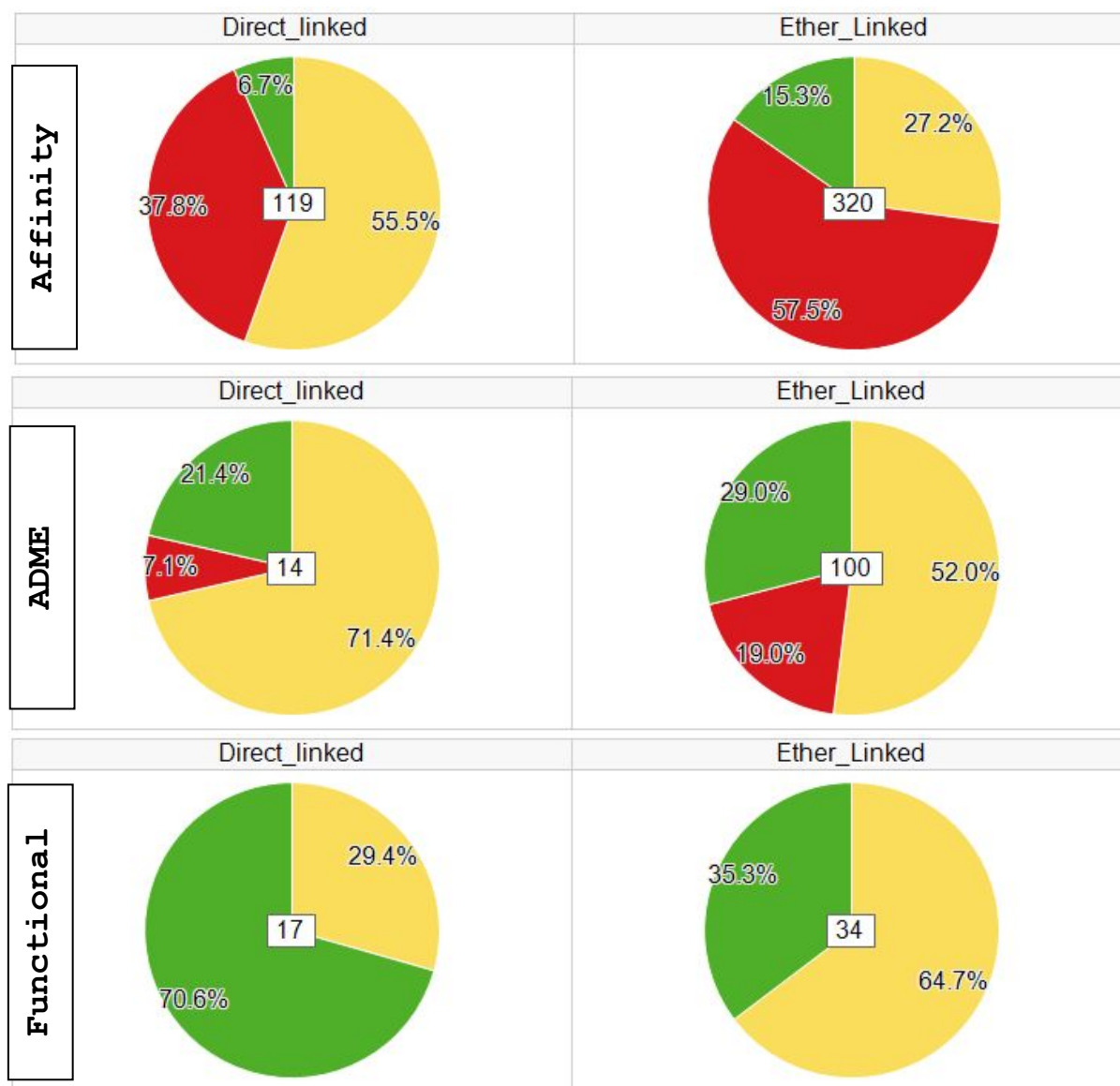
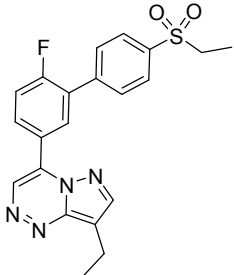
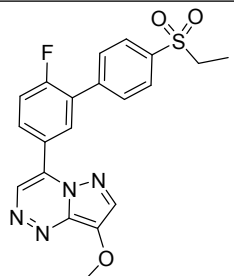
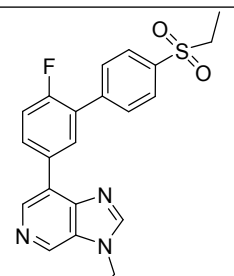
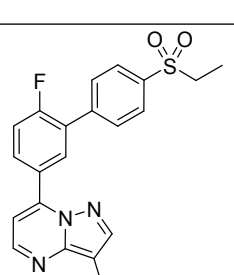


Figure 3. Probability analysis of two main subseries within Series 2 on the basis of: **Affinity:** α_2 K_i < 10 nM Green, >40 nM Red. **ADME:** HLM < 20 AND MDR er < 2.5 Green, HLM > 40 AND MDR er > 4.0 Red. **Functional:** α_1 PCT < 20 and α_2 PCT > 50 Green, α_1 PCT > 50 AND α_2 < 40 Red

FINAL OPTIMIZATION AND IDENTIFICATION AND CHARACTERIZATION OF PRECLINICAL LEADS

With our design strategy focused on the imidazopyridazine series, the project team next explored a few different core modifications in order to determine if there were any advantages to alternative heterocyclic cores (Table 5). Modification of compound **22** to a pyrazolotriazine (**28**) provided a boost in affinity and efficiency while maintaining the desired functional selectivity. This core was particularly interesting as it provided access to different substituents in the lower right quadrant that were not accessible for the imidazopyridazine scaffold, for example compound **29**. Unfortunately, this series was generally less stable than the imidazopyridazine series and a majority of the compounds were highly coloured, typically bright yellow or orange, leading to concerns of photostability and was therefore not explored further. Compounds **30** and **31** demonstrated that both nitrogens of the pyridazine ring system were required for good binding affinity. Finally, the triazolopyridazone core was tolerated but as it was less efficient than the imidazopyridazine, was also not explored further. Although ultimately unproductive, this work allowed the project team to confidently focus on the imidazopyridazine core in our final rounds of optimization.

Structure	ID	$\alpha 2$ Ki \pm SEM (nM)	Lip E ^a	$\alpha 1$ PAM \pm SEM (%) ^b	$\alpha 2$ PAM \pm SEM (%) ^c	LogD ^d	HLM ^e Clint (μ L/min/mg)	MDR ^f
	28	2.8 \pm 1.8 (n=3)	5.1	9 \pm 5 (n=2)	71 \pm 4 (n=2)	3.5	33	1.1
	29	29.7 \pm 5 (n=4)	4.7	-13 \pm 3 (n=11)	77 \pm 4 (n=13)	2.8	<8	1.8
	30	655.9 (n=1)	2.9	ND	ND	3.3	ND	ND
	31	944.3 \pm 162.2 (n=2)	2.1	ND	ND	3.9	30	2.1

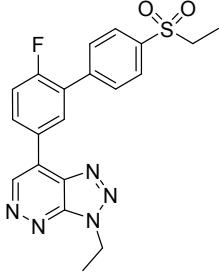
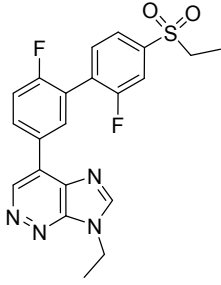
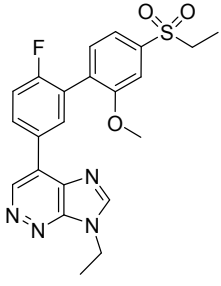
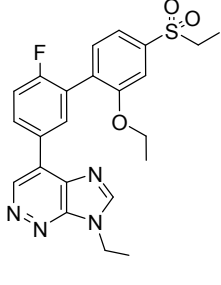
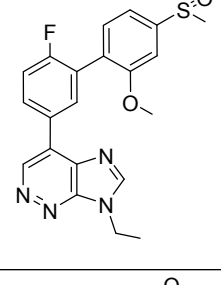
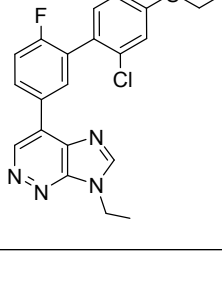
	32	81.3 ± 17.1 (n=3)	3.8	-1 ± 1 (n=5)	107 ± 18 (n=7)	3.3	25	1.4
-----------------------------------------------------------------------------------	-----------	-------------------------	-----	--------------------	----------------------	-----	----	-----

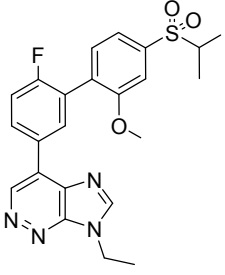
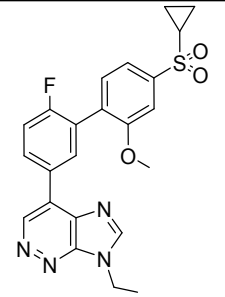
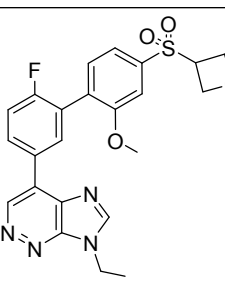
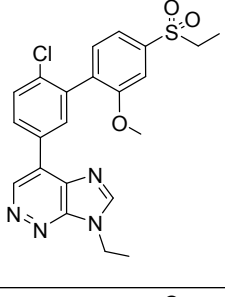
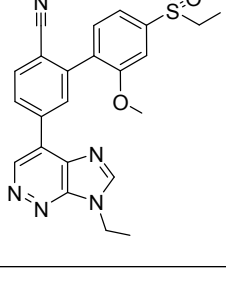
Table 5. The effect of modification to the imidazopyridazine core. ^aLogD are measured values or if calculated (internal logD model) are in italics. ^{b,c}GABA_A functional activity were measured at 100-times the compound's IC₅₀. ^dLipE values are calculated (pIC₅₀ - logD) from measured logD values when possible or from calculated logD. ^eHLM Clint (μL/min/mg), in vitro human microsomal stability measurement. ^fMDR er: Ratio from the MS-based quantification of apical/basal and basal/apical transfer rates of test compound at 2 μM across confluent monolayers from MDR1-transfected MDCK cells.

Two compounds stood out from the optimization work outlined in Table 4, the sulfone containing compound **22** and the amide containing compound **26**. Compound **22** exemplified the desired functional and ADME profile but ideally could have higher affinity. In contrast, compound **26** had the desired level of affinity, but was not ideal in terms of functional selectivity and CNS penetration based on its MDR ratio. Focusing first on optimizing affinity for compound **22**, combining SAR from the above studies, namely the affinity improvement observed by

introducing an ortho-fluoro group (**22** to **23**), compound **33** was synthesized. Unfortunately, this modification did not yield an improvement in affinity. However, increasing the size of the fluoro group to a methoxy group (**34**) did provide a large improvement in both affinity and efficiency. This compound also maintained an excellent level of functional selectivity and a desirable ADME profile. Small changes to the structure of compound **34** suggested that the ethyl sulfone and methoxy groups were optimal. Attempts to increase the size of the methoxy group (**35**), change the electronics of the ring system (**37**) or decrease (**36**) or increase (**38**) the size of the sulfone were all detrimental to the functional profile. The best alternative to compound **34** in terms of functional selectivity was the cyclopropyl containing compound **39**, but this modification led to a drop in affinity. The fluorophenyl group central ring system also appeared to be optimal with replacement of the fluorine with either a chlorine or a nitrile leading to a reduction in affinity and some erosion of the functional selectivity. This work suggested that within the sulfone series, compound **34** was the optimal compound to profile further.

Structure	ID	$\alpha 2$ Ki \pm SEM (nM)	Lip E ^a	$\alpha 1$ PAM \pm SEM (%) ^b	$\alpha 2$ PAM \pm SEM (%) ^c	LogD ^d	HLM ^e Clint (μ L/min/mg)	MDR ^f
-----------	----	------------------------------	--------------------	-------------------------------------------	-------------------------------------------	-------------------	------------------------------------------------	------------------

	33	18.2 ± 5.4 (n=4)	5.2	-31 ± 2 (n=9)	43 ± 2 (n=15)	2.6	<8	1.6
	34	2.9 ± 3.7 (n=8)	5.9	21 ± 2 (n=21)	134 ± 3 (n=34)	2.7	<9	1.8
	35	18.4 ± 2.4 (n=4)	4.4	67 ± 8 (n=11)	129 ± 17 (n=13)	3.3	12	1.7
	36	7.5 ± 1.8 (n=6)	5.6	6 ± 2 (n=17)	45 ± 4 (n=15)	2.5	<8	3.3
	37	7.3 ± 1.6 (n=4)	5.0	-7 ± 3 (n=8)	14 ± 2 (n=12)	3.2	9	1.8

	38	11.6 ± 1.1 (n=6)	5.0	40 ± 6 (n=15)	111 ± 5 (n=19)	3.0	84	1.5
	39	12.7 ± 2.2 (n=4)	5.1	27 ± 6 (n=4)	115 ± 5 (n=4)	2.7	<12	2.6
	40	6.6 (n=1)	6.0	58 ± 6 (n=3)	171 ± 10 (n=5)	2.2	67	7.0
	41	29.7 ± 5.3 (n=4)	4.4	22 ± 3 (n=12)	77 ± 7 (n=20)	3.1	<8	2.9
	42	40.6 ± 3 (n=4)		21 ± 2 (n=13)	84 ± 12 (n=13)		<8	4.0

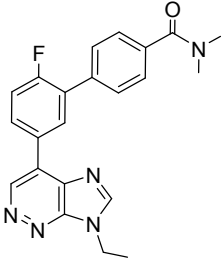
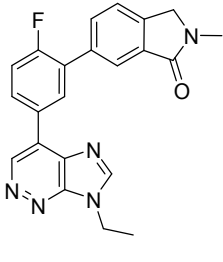
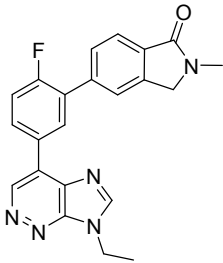
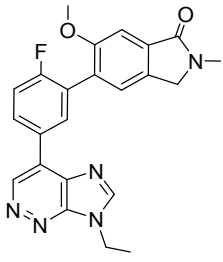
	43	71.6 ± 12.3 (n=2)	4.7	-14 ± 5 (n=7)	13 ± 3 (n=8)	2.5	13	1.8
	44	21.7 ± 6.2 (n=3)	5.1	-29 ± 2 (n=10)	43 ± 3 (n=12)	2.6	77	1.7
	45	12.8 ± 5.3 (n=4)	5.2	-30 ± 3 (n=8)	47 ± 2 (n=9)	2.7	34	1.5
	46	6.6 ± 1.4 (n=10)	5.6	-27 ± 2 (n=25)	96 (n=33)	2.6	14	3.1

Table 6. Optimization of direct linked aryl-based imidazopyridazine subseries. α_2 Ki and α_1/α_2 PAM values were measured as described here.³³⁻³⁵ ^aLogD are measured values or if calculated (internal logD model) are in italics. ^{b,c}GABA_A functional activity were measured at 100-times the compound's IC₅₀. ^dLipE values are calculated (pIC₅₀ - logD) from measured logD values when possible or from calculated logD. ^eHLM Clint (μL/min/mg), in vitro human microsomal stability measurement.

^fMDR er: Ratio from the MS-based quantification of apical/basal and basal/apical transfer rates of test compound at 2 μ M across confluent monolayers from MDR1-transfected MDCK cells.

In the context of optimizing the ADME and functional profile of compound **26**, the project team initially synthesized compound **43**, which demonstrated that the MDR efflux ratio could be improved through removing a hydrogen bond donor. This modification did not improve the functional profile and decreased affinity, however constraining the amide in two different orientations via lactams **44** and **45**, yielded compounds that were comparable to compound **26**. Based on the affinity enhancement seen for compound **34** relative to **22**, an ortho-methoxy group was introduced to yield compound **46**. This modification led to a small improvement in affinity, but more importantly led to an increase in α 2 functional activity which yielded a compound that met our criteria for functional selectivity. In addition, while slightly less active at α 2, the inverse activity of **46** at α 1 provides a compound with GABA_A pharmacology profile that complemented compound **34**. Compound **46** carried some risk of CNS-restriction based on the MDR efflux ratio, but not enough to preclude further evaluation. Based on these results, it was decided to advance both compounds into further in vitro and in vivo studies.

GABA_A Pharmacology

The affinity (K_i) of compounds **34** and **46** for the benzodiazepine site of GABA_A receptors was then determined in radioligand competition binding experiments against receptors containing a range of different α -subunits.³⁶ Compounds **34** and **46** were determined to be high affinity ligands at GABA_A receptors containing $\alpha 1$, $\alpha 2$, $\alpha 3$ or $\alpha 5$ subunits (Table 7), but had very low affinity for GABA_A receptors containing $\alpha 4$ or $\alpha 6$ subunits, which is typical for ligands that bind at the benzodiazepine binding site. Interestingly, in contrast to the functional efficacy values reported earlier, both compound **34** and **46**, exhibited greater binding affinity for the $\alpha 1$ -containing receptor compared with $\alpha 2$ -containing receptors. Although the higher affinity at $\alpha 1$ for both compounds may result in greater receptor occupancy relative to $\alpha 2/3$ containing receptors for a given dose, it was anticipated that the inverse selectivity would not result in undesirable side-effects due to the very low level of allosteric modulation.

The functional activity of compounds **34** and **46** were also determined in electrophysiological experiments using the same recombinant cell lines used for the binding studies. An open channel QPatch based assay format was used in which GABA_A

receptors were opened using an EC₁₀ concentration of GABA and then compound was applied and potentiation measured.³⁶ The data showed that compounds **34** and **46** exhibited subtype-selectivity for GABA_A receptors containing $\alpha 2$, $\alpha 3$, and $\alpha 5$ subunits and had negligible (**34**) or slightly negative (**46**) activity at GABA_A receptors containing $\alpha 1$ subunits. Similar functional data was generated using manual patch techniques, thereby confirming the validity of the higher throughput QPatch methods. In addition, neither of these compounds exhibited any species selectivity between rat and human derived receptors. While the in vitro efficacy of **34** and **46** is lower than that of precededented clinical benzodiazepines such as diazepam (% $\alpha 2$ modulation of 134% and 93% respectively for **34** and **46** vs 293% for diazepam; see tables 6 and 1 respectively), it was assumed that the reduction or removal of $\alpha 1$ mediated side effects would mean this could be compensated for by achieving higher levels of $\alpha 2$ receptor occupancy. Both preclinical and early clinical data supported this assumption with robust measures of pharmacodynamic effects being observed (vida infra).³⁶

Property	Compound 34	Compound 46 (n, 95% CI)
Human GABA _A Ki (nM)	(n, 95% CI)	(n, 95% CI)
$\alpha 1\beta 3\gamma 2$	0.18 (5, 0.1-0.4)	0.64 (6, 0.2-0.5)
$\alpha 2\beta 2\gamma 2$	2.9 (8, 1.0-8.2)	6.6 (10, 4.8-

		11.2)
$\alpha 3\beta 3\gamma 2$	1.1 (6, 0.6-2.0)	2.5 (5, 0.5-5.7)
$\alpha 4\beta 3\gamma 2$	>19900 (6)	ND
$\alpha 5\beta 2\gamma 2$	18 (6, 7.3-45)	33 (6, 22-48)
$\alpha 6\beta 3\gamma 2$	>19900 (6)	>19900 (5)
Human GABA_A functional activity		
(% enhancement) (QPatch/Manual Patch)	(n, \pm SEM)	(n, \pm SEM)
$\alpha 1\beta 3\gamma 2$	21 (21, 2) / 20 (8, 3)	-27 (25, 2)
$\alpha 2\beta 3\gamma 2$	134 (34, 3) / 124 (7, 12)	96 (33, 4)
$\alpha 3\beta 3\gamma 2$	92 (22, 5) / 92 (22, 20)	56 (20, 5)
$\alpha 5\beta 3\gamma 2$	91 (22, 4) / 95 (7, 12)	61 (21, 5)
Rat GABA_A Ki (nM)		
	(n, 95% CI)	(n, 95% CI)
$\alpha 1\beta 3\gamma 2$	0.34 (5, 0.1-0.9)	0.5 (6, 0.4-0.8)
$\alpha 2\beta 2\gamma 2$	4.58 (6, 2.1-10.1)	ND
Rat GABA_A functional activity (% enhancement)		
	(n, \pm SEM)	(n, \pm SEM)
$\alpha 1\beta 3\gamma 2$	0.6 (11, 3.4)	-26 (22, 2.6)
$\alpha 2\beta 2\gamma 2$	54 (12, 6)	36 (19, 3.1)

Table 7. Affinity and efficacy profiles of compound 34 & compound 46 in rat and human. Ki values were determined in membranes prepared from recombinant cells heterologously expressing given GABA_A receptor subtypes. [3H]Ro15-1788 was used to determine affinity at GABA_A receptors containing $\alpha 1$, $\alpha 2$, $\alpha 3$, or $\alpha 5$ subunits and [3H]Ro15-4513 was used to determine affinity at GABA_A receptors containing $\alpha 4$ or $\alpha 6$ subunits.

Pharmacokinetics, CNS distribution and In Vivo Efficacy

In addition to the pharmacology profiling describe above, compounds 34 and 46 were also profiled through a range of in vitro ADME assays to confirm their suitability for further progression. Both compounds had physicochemical profiles that were generally consistent with good CNS permeability.¹⁹⁻²¹ In

addition, both compounds demonstrate suitable in vitro profiles including good metabolic stability across human, rat and dog hepatocyte and microsome preparations as well as minimal P-gp or BCRP mediated efflux. While compound **34** showed a potential to inhibit P-gp and BCRP it was not thought that this would prohibit development given low target concentrations. Neither compound showed any appreciable risks with regards to other drug-drug interactions (DDI). These data suggested that both compounds would exhibit sufficient oral and CNS exposure in vivo, and therefore were progressed into in vivo studies to determine their preclinical pharmacokinetic and CNS distribution.

Property	Compound 34	Compound 46
<i>Physicochemical properties</i>		
Molecular weight (Da)	440.5	417.4
clogP	2.7	2.5
HBD/HBA	0 / 6	0 / 5
Sum N+O	7	7
logD	2.7	2.6
TPSA (Å)	95	73
CNS MPO	5.1	5.3
Solubility at pH6.5 (µM)	95	15
<i>ADME in vitro profiles</i>		
RRCK ³⁷ (x 10 ⁻⁶ cm/sec)	17	21
P-gp efflux ratio	1.8	3.1
BCRP efflux ratio	ND	2.5
HLM, Cl _{int} (µL/min/mg)	<9	14
RLM, Cl _{int} (µL/min/mg)	<14	<14
DLM, Cl _{int} (µL/min/mg)	27	27
HHEP, Cl _{int} (µL/min/10 ⁶ cells)	6	11
RHEP, Cl _{int} (µL/min/10 ⁶ cells)	15	11
DHEP, Cl _{int} (µL/min/10 ⁶ cells)	45	22
hppb fu	0.128	0.79
rppb fu	0.073	0.028
dppb fu	0.107	0.18

Human Blood to Plasma Ratio	2.3	0.9
Rat Blood to Plasma Ratio	1.5	0.6
Dog Blood to Plasma Ratio	3.2	0.8
Transporter inhibition		
hOAT1 (μM)	>5	ND
hOAT3 (μM)	>5	ND
hOCT2 (μM)	>5	ND
P-gp (μM)	1.1	ND
BCRP (μM)	3.6	ND
Cyp Inhibition		
CYP1A2, inh. IC ₅₀ (μM)	>150	>30
CYP2B6, inh. IC ₅₀ (μM)	77	ND
CYP2C8, inh. IC ₅₀ (μM)	52	15.2
CYP2C9, inh. IC ₅₀ (μM)	11	14.5
CYP2C19, inh. IC ₅₀ (μM)	40	22.8
CYP2D6, inh. IC ₅₀ (μM)	82	>30
CYP3A4, inh. IC ₅₀ (μM)	>50 ¹	>30

Table 8. Broader in vitro ADME profiles of lead compounds compound 34 & compound 46. ¹Tested against three substrates.

The preclinical pharmacokinetic profiles of compound **34** and **46** were determined in both rat and dog (Table 9). Compound 34 exhibited moderate plasma clearance (Clp) of 22 mL/min/kg (liver blood flow value 70 mL/min/kg) in rat, which coupled to a steady state volume of distribution (V_{ss}) of 2.1 L/kg, resulted in a short terminal half-life (t_½) of 1.1 hours. Compound **46** had a lower V_{ss} in rats than **34** (0.551 L/kg), but also showed lower clearance (2.20 mL/min/kg), so ultimately exhibited a longer terminal half-life of 4 hours. Both compounds had similar in vivo PK profiles in dog with plasma clearance rates around 75% liver blood flow (29 and 33 mL/min/kg) and moderate V_{ss} values which resulted in short terminal half-lives (0.9 and 0.75 h). In addition, both compounds also had high bioavailability in

both rat and dog In the case of compound **34** it should be noted that blood:plasma ratio in dog was 3.2 leading to a lower blood clearance value more in keeping with the observed high bioavailability.

Property	Compound 34	Compound 46
Rat PK		
Clp (mL/min/kg)	22	2.20
T1/2 (h)	1.1	4.0
Vss (L/kg)	2.1	0.55
F (%)	99	76
Dog PK		
Clp (mL/min/kg)	29	33
T1/2 (h)	0.9	0.75
Vss (L/kg)	3.4	2.61
F (%)	130	43
Rat RO		
Occ ₅₀ Plasma total (ng/ml)	51.8	513.1
Occ ₅₀ Forebrain total (ng/g)	32.3	35.8
Occ ₅₀ Spinal Cord total (ng/g)	30.9	74.4
Occ ₅₀ Cerebellum total (ng/g)	7.6	18.4
Occ ₅₀ Plasma unbound (nM)	8.5	34.4
Mouse RO		
Occ ₅₀ Plasma total (ng/ml)	141.4	
Occ ₅₀ Brain total (ng/g)	160.9	
Occ ₅₀ Spinal Cord total (ng/g)	134.2	
Occ ₅₀ Plasma unbound (nM)	26.7	

Table 9. Preclinical PK and RO results for compound 34 & compound 46. Occ₅₀ - dose required to produce 50% occupancy

Both compounds were then progressed to in vivo studies in rodents to confirm that each could effectively engage the target. Compounds 34 and 46 both showed a dose-dependent increase in RO in forebrain, spinal cord and cerebellum as measured by displacement of the radioligand [3H]Ro15-1788 (flumazenil) (Table 10). Both compounds had unbound plasma OC_{50} values that were comparable to their respective in vitro $\alpha 1$ and/or $\alpha 2$ binding K_i values (Table 7). Compound **46** seem to exhibit a small amount of impairment which may have been a result of the slightly higher P-gp efflux ratio, but neither compound exhibits any significant CNS impairment in preclinical species that precluded its further advancement. Interestingly, both compounds showed some variation in RO across the three tissues measured. This variation was expected due to enrichment of the $\alpha 1$ subunit in the cerebellum,² as the compounds exhibited binding-selectivity for the $\alpha 1$ subunit.

Finally, both compounds were profiled in a range of different efficacy experiments to confirm that they exhibited the desired GABA_A pharmacology in vivo. As can be seen in Table 10 (and expanded on in SI), both compound **34** and **46** demonstrated efficacy in a chronic constriction injury (CCI) model of neuropathic pain. Compound **34** exhibited efficacy in two models of epilepsy, PTZ induced seizures and amygdala kindling.

Compound **46** only exhibited a trend towards seizure reduction in a PTZ model, which we considered to be reflective of the different methodologies used in the two studies. Compound **46** also exhibited efficacy in a mouse elevated plus maze model of anxiety. As a result of these data, both compounds were deemed suitable for further progression with both having a high probability of exhibiting the desired GABA_A-related pharmacology in humans.

Model	Compound 34		Compound 46	
	Dose (mg/kg)	Results	Dose (mg/kg)	Results
CCI model (rat)	3, 10	Both doses significantly increased paw withdrawal latency	10, 30	Both doses significantly increased paw withdrawal latency
PTZ seizure model (mouse)	0.3, 3, 10	All doses significantly increased seizure latency	1, 10, 30	Trend to increase seizure latency
Amygdala kindling (rat)	1, 3, 10	All doses exhibited efficacy on some parameters	N.D.	N.D.
Elevated plus maze (mouse)	0.1, 0.32, 1, 3.2, 10	Anxiolytic activity observed at 3.2 and 10mg/kg	N.D.	N.D.

Table 10. Results from in vivo efficacy studies for compound 34 & compound 46.

IN VITRO AND PRECLINICAL SAFETY STUDIES

In parallel to the studies described above, compounds **34** and **46** were profiled in a range of in vitro safety studies (Table 11). In terms of other off target activity, with the exception of the NK2 receptor and the benzodiazepine site of the GABA_A receptor, Compound **34** did not inhibit ligand binding activity by more than 50% at 10 μ M at any of the binding sites in the CEREP panel, showing limited off-target pharmacology. Follow up screening of **34** at NK2 demonstrated an IC₅₀ 21 μ M, which provided a large margin above anticipated clinical levels. Similar screening for compound **46** had activity at Abl Kinase (8.7 μ M) and PDE4D2 (6.6 μ M), again having a high margin of coverage over projected clinical unbound concentrations. The cytotoxicity potential of both compounds was evaluated in the THLE³⁸ cell line with Compound **34** showing an IC₅₀ of 12.9 μ M IC₅₀ compared to 159.7 μ M with Compound **46**. Both compounds were negative in the Ames mutagenicity test, but positive in the in vitro micronucleus assay (IVNM) assay, with follow up testing indicating these positive results were caused by aneugenic activity, a potential risk that can be managed during clinical development. In 14-day exploratory toxicity studies in both the rat and dog, compound **34** (PF-06372865) exhibited no findings that precluded its progression into further toxicity studies and ultimately clinical studies.³⁶ Unfortunately, although compound **46** (PF-06659286) was well tolerated in the rat, this compound caused

hepatic related findings in the dog at all doses tested and was therefore not pursued further.

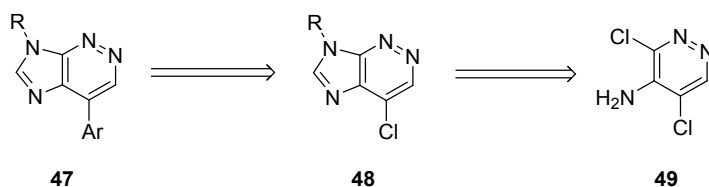
Property	Compound 34	Compound 46
<i>CEREP Off Target Pharmacology</i> ¹	NK2 IC ₅₀ = 21μM	Abl IC ₅₀ = 8.7μM
		PDE4D2 IC ₅₀ = 6.6μM
hERG ephys. IC ₅₀ (μM)	26.8	>30
Nav1.5 IC ₅₀ (μM)	>100	>100
THLE (μM)	12886	159668
IVMN (+/- S9)	Aneugen	Aneugen
Ames	Negative	Negative

Table 11. Preclinical In vitro Safety for compounds compound 34 & compound 46. ¹Each compound was screened in a panel of >140 off target binding assays (<http://www.cerep.fr/cerep/users/pages/ProductsServices/bioprntservices.asp>)

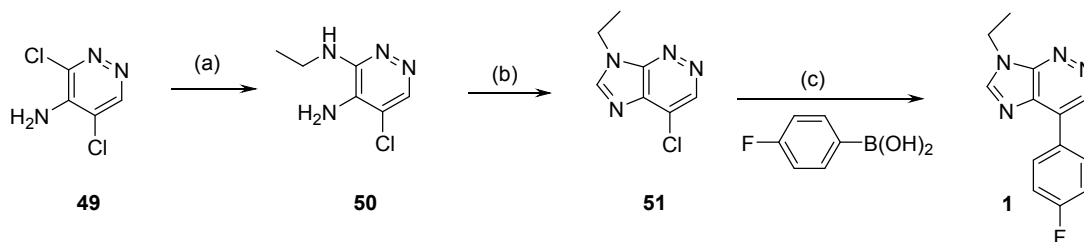
SYNTHETIC ROUTES

Our basic disconnection strategy is shown in Scheme 1. A range of aryl imidazopyridazines **47** could be readily made by Suzuki coupling on chloroimidazopyridazine **48** which itself could be constructed from 3,5-dichloropyridazin-4-amine **49**. Amine **49** was accessible using the method of Kelley.³⁹ This strategy was successfully utilized in the synthesis of (**1**) (Scheme 2).

Scheme 1. Retrosynthetic route to aryl imidazopyridazines.



Scheme 2. Synthesis of imidazopyridazine **1**.

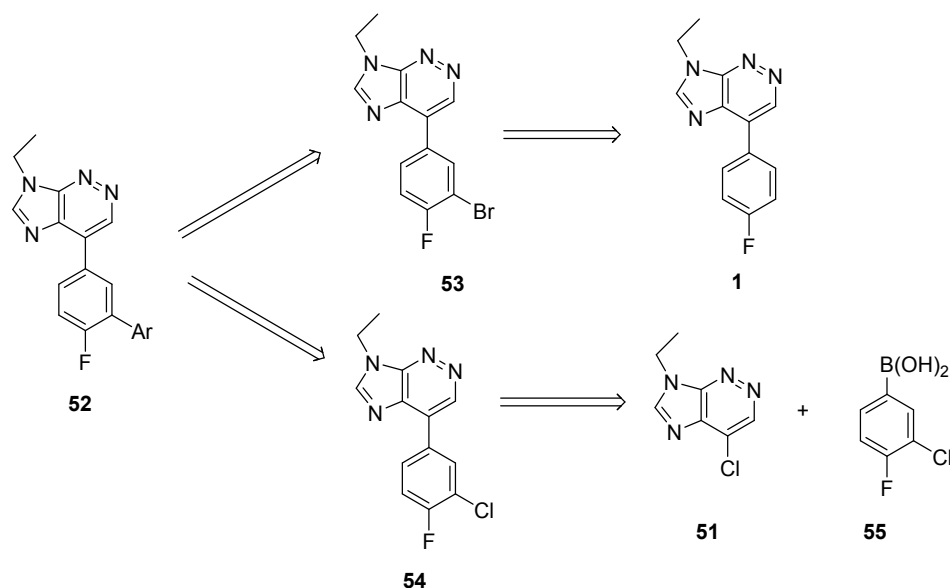


Reagents and conditions: (a) EtNH_2 , H_2O , $120\text{ }^\circ\text{C}$, 48h, 51%. (b) $\text{HC}(\text{OEt})_3$, $130\text{ }^\circ\text{C}$, 4h, 45%. (c) $\text{Pd}(\text{PPh}_3)_4$, Cs_2CO_3 , dioxane, H_2O , $100\text{ }^\circ\text{C}$, 16h, 70%.

Amine **49** was heated to $120\text{ }^\circ\text{C}$ for 48 hours with ethylamine (70% solution in water) to give diamine **50** regioselectively. Heating the diamine with ethyl orthoformate at $130\text{ }^\circ\text{C}$ resulted in the formation of the desired chloroimidazopyridazine **51**. Suzuki-Miyaura coupling of **51** with (4-fluorophenyl)boronic acid using $\text{Pd}(\text{PPh}_3)_4$ as catalyst and cesium carbonate as base gave the desired target molecule **1** in excellent yield.

Compounds with additional aryl groups on the fluoroaromatic ring **52** were typically synthesized from the 3-bromo-4-fluorophenyl imidazopyridazine **53** or the 3-chloro-4-fluoro derivative **54** (Scheme 3).

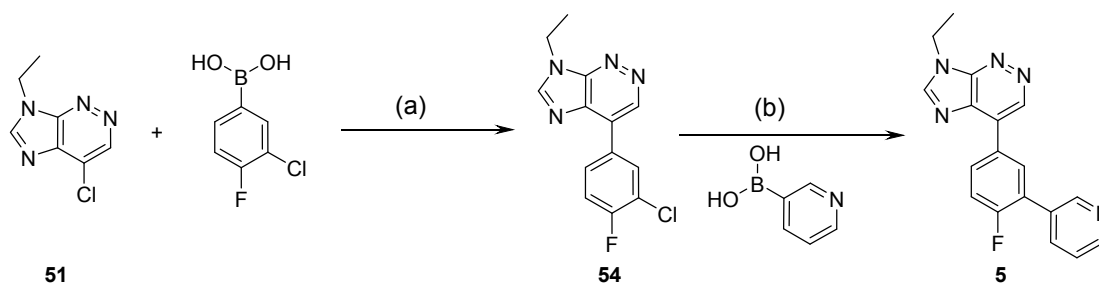
Scheme 3. General routes to 3- aryl, 4-fluoro substituted imidazopyridazines.



The use of aryl bromide **53**, allowed the Suzuki coupling to be carried out under reasonably mild conditions while more electron-rich sterically hindered ligand systems were typically needed for reactions of aryl chloride **54**. However, while bromide **53** was most effectively synthesized by bromination of **1**, chloride **54** could be made directly by Suzuki coupling of **48** with the (3-chloro-4-fluorophenyl)boronic acid **55**.

For example, the 3-pyridyl variant **5** could be synthesized through Suzuki coupling of 3-pyridyl boronic acid with aryl chloride **54** but effective coupling required the use of the sterically demanding and electron-rich catalyst $\text{Pd}(\text{dtbpf})\text{Cl}_2^{40}$ (Scheme 4).

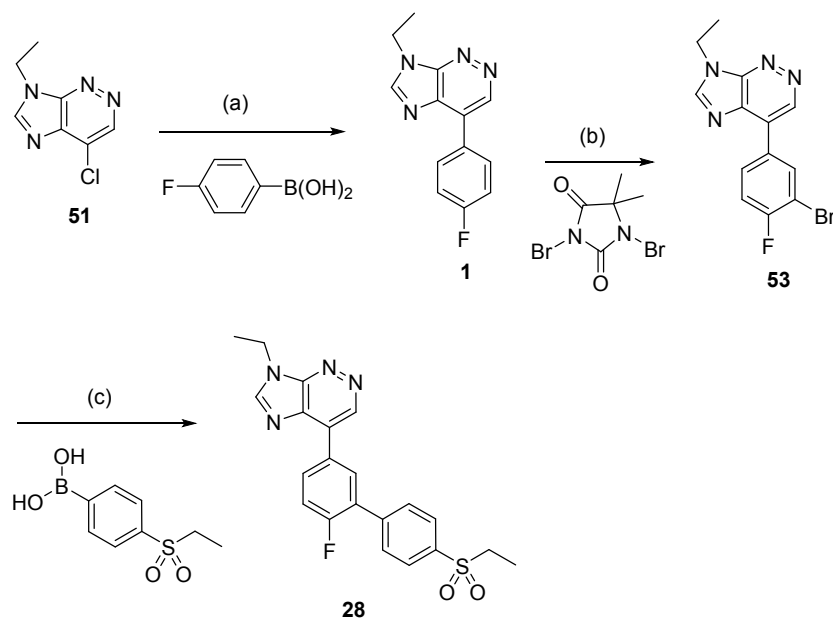
Scheme 4. Synthesis of 3-pyridyl, 4-fluoro imidazopyridazine.



Reagents and conditions: (a) $\text{Pd}(\text{PPh}_3)_4$, Cs_2CO_3 , dioxane, H_2O , 100 °C. (b) $\text{Pd}(\text{dtbpf})\text{Cl}_2$, Cs_2CO_3 , dioxane, H_2O , 100 °C, 38% over 2 steps.

In contrast, sulfone **28** was synthesized from aryl bromide **53**; here, the use of $\text{Pd}(\text{PPh}_3)_4$ in the Suzuki coupling gave an excellent yield of desired product. Bromide **53** was synthesized from fluorophenyl imidazopyridazine **1** using the strongly electrophilic bromination conditions of 1,3-dibromo-5,5-dimethylhydantoin and concentrated sulphuric acid⁴¹ (Scheme 5).

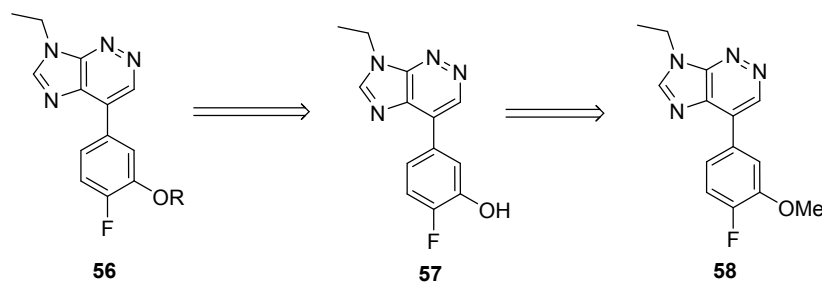
Scheme 5. Synthesis of sulfones.



Reagents and conditions: (a) $\text{Pd}(\text{PPh}_3)_4$, Cs_2CO_3 , dioxane, H_2O , 100°C , 55% . (b) H_2SO_4 , 0°C , 41%. (c) $\text{Pd}(\text{PPh}_3)_4$, Cs_2CO_3 , dioxane, H_2O , 100°C , 73% .

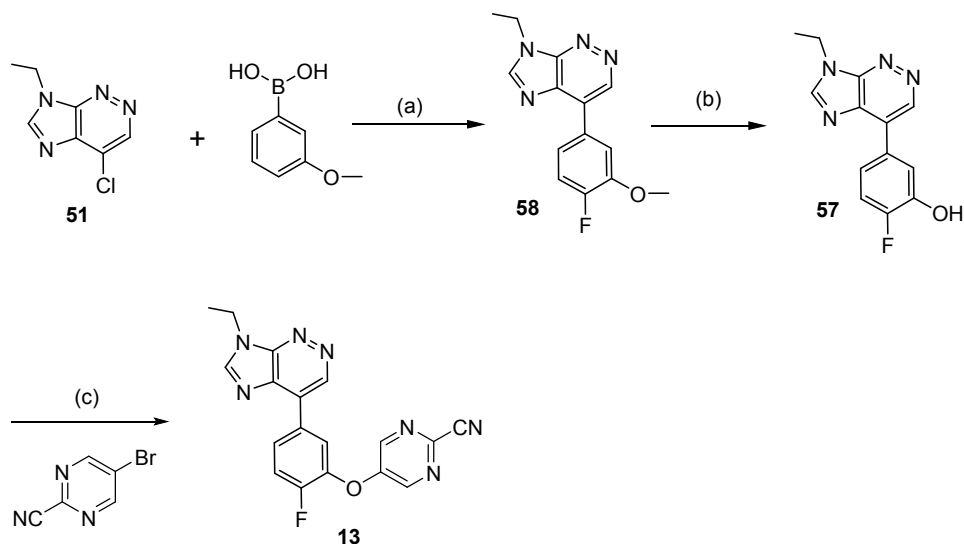
Fluoroalkoxy derivatives were accessed using the approach shown in Scheme 6. Key to this approach was the demethylation of fluoromethoxy variant (**58**) to give the required phenol (**57**). The phenol could then be alkylated or arylated. This method was used for parallel synthesis of these analogs, using **57** as a common intermediate for SAR expansion.

Scheme 6. General route to fluoroalkoxy/aryloxy imidazopyridazines.



This approach was applied in the synthesis of **13**.

Scheme 7. Synthesis of Compound **13**.

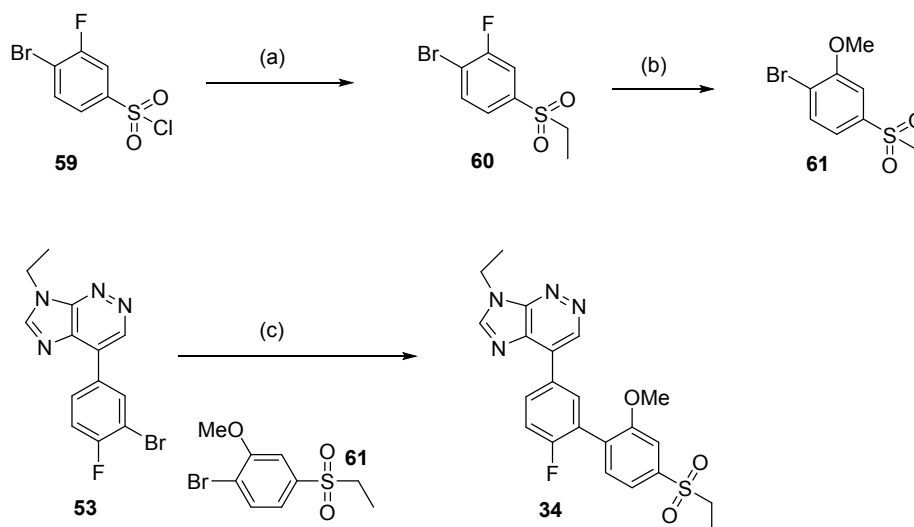


Reagents and conditions: (a) $\text{Pd}(\text{dtbpf})\text{Cl}_2$, Cs_2CO_3 , dioxane, H_2O , 100°C , 42%. (b) BBr_3 , DCM , 51%. (c) K_2CO_3 , DMF , 50°C , 2h (in parallel).

Suzuki-Miyaura coupling of (3-methoxyphenyl)boronic acid with chloroimidazopyridazine **51** was carried out in good yield using $\text{Pd}(\text{dtbpf})\text{Cl}_2$ and cesium carbonate to give the fluoromethoxyphenyl imidazopyridazine **58**. Demethylation could be carried out effectively using boron tribromide in dichloromethane to give phenol **57**. This intermediate was used for parallel synthesis, thus subsequent $\text{S}_\text{N}\text{Ar}$ reaction with 5-bromo-2-cyanopyrimidine gave bromopyrimidine **13** after automated purification.

Utilising the methods discussed above, two compounds were selected for scale-up. Ethyl sulfone **34** was synthesised as shown in Scheme 8.

Scheme 8. Synthesis of sulfone **34**.



Reagents and conditions: (a) (i) N₂H₄, THF. (ii) EtI, NaOAc, EtOH, reflux, 64%. (b) NaOMe, MeOH, 100 °C, 75%. (c) (i) (BPin)₂, KOAc, Pd(dppf)Cl₂, dioxane, 100 °C. (ii) Na₂CO₃ (aq), Pd(dppf)Cl₂, 100 °C, 80%.

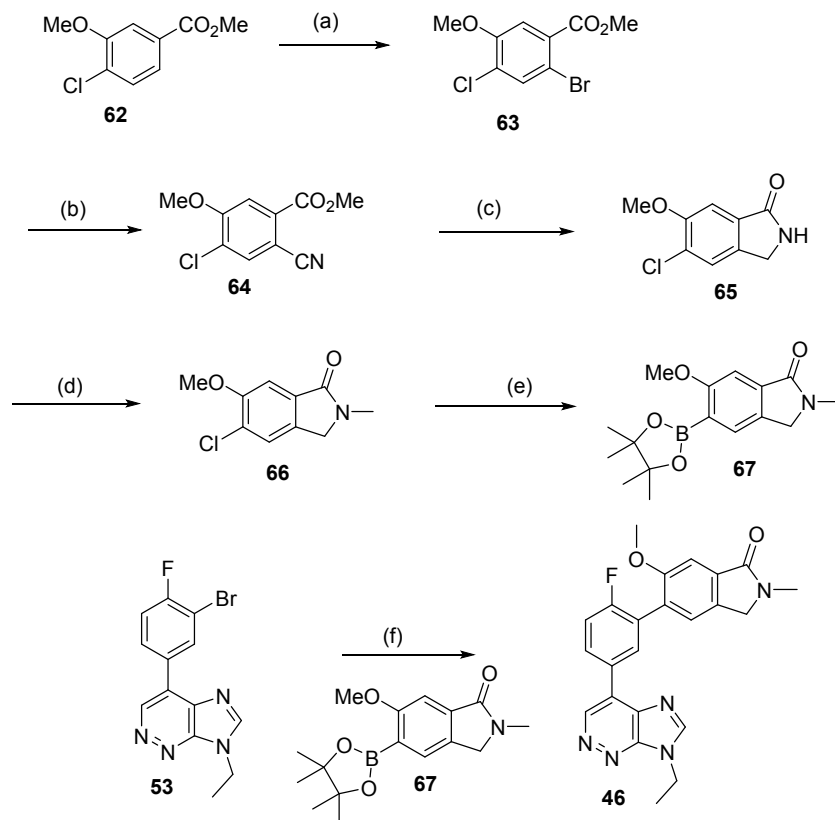
1-bromo-4-(ethylsulfonyl)-2-methoxybenzene **61** could be readily synthesised from 4-bromo-3-fluorobenzenesulfonyl chloride **59**. Reaction of the sulfonyl chloride **59** with hydrazine formed the sulfonyl hydrazide. Reaction of the hydrazide with ethyl iodide and sodium acetate in ethanol at reflux converted it through to the ethylsulfone (the reaction occurring through alkylation and elimination under the basic conditions to give the sulfinate which is subsequently alkylated with the ethyl iodide) to give **60**.⁴² In order to effect Suzuki-Miyaura coupling, the 3-bromo-4-fluorophenyl imidazopyridazine **53** was converted to the B(Pin) ester using (BPin)₂, Pd(dppf)Cl₂ and potassium acetate in dioxane under reflux conditions. While the boronate ester could be

isolated at this point, it proved more effective to utilise a "one-pot" approach to obtain **34** on scale. After conversion to the B(Pin) ester was complete, the mixture was allowed to cool and then further base (aqueous 2M sodium carbonate solution) was added together with additional Pd(dppf)Cl₂. The ethyl sulfone **61** was then added and the mixture was refluxed until reaction was complete. This two step, one-pot method allowed **34** to be isolated in 80% yield.

Methoxylactam **46** was synthesised as shown in Scheme 9. Methyl 4-chloro-3-methoxybenzoate **62**. was brominated regioselectively in good yield with bromine in acetic acid to give **63**. Cyanation of **63** initially proved low yielding but trituration of the starting bromide with ethanol allowed the reaction to proceed in high yield. The key reaction in the sequence was the formation of the lactam **65** from the cyanide **64**. This was carried out with Raney Nickel and ammonia under hydrogen in an ethyl acetate/methanol mixture. However, these conditions did lead to considerable dechlorination of the resulting lactam and this side product proved inseparable from the desired lactam **65**. This was carried forward as a mixture. Chlorolactam **65** was subsequently alkylated with sodium hydride and methyl iodide to form **66** and then converted to the boronate ester **67** using (BPin)₂, Pd₂(dba)₃ and PCy₃. Coupling of boronate **67** with 3-

bromo-4-fluorophenyl imidazopyridazine **53** occurred in modest yield to give the desired methoxy lactam **46**.

Scheme 9. Synthesis of lactam **46**.



Reagents and conditions: (a) Br_2 , AcOH, H_2O , 60°C , 87%. (b) CuCN , DMF, 150°C , 83%. (c) RaNi , DMAc, AcOH, H_2 , 45 PSI, 71%. (d) NaH , MeI, THF, 0°C - rt, 91%. (e) $(\text{BPin})_2$, KOAc, $\text{Pd}_2(\text{dba})_3$, Cy_3P , dioxane, 110°C , 94%. (f) $\text{Pd}(\text{PPh}_3)_4$, Na_2CO_3 , dioxane, H_2O , 100°C , 37%.

Given the issue of dechlorination in the formation of the lactam **65**, we examined the key hydrogenation step in more detail. We found that the use of Raney Nickel and acetic acid in DMAc gave excellent yields of the desired product **65** without

loss of the chlorine from the product (reported in Scheme 9). While this would have undoubtedly resulted in higher yields in the final coupling step, it was not pursued further as an improved coupling route was developed for further larger scale synthesis. These results will be reported in due course.

CONCLUSIONS

In summary, a series of imidazopyridazine-based, subtype-selective PAMs for the GABA_A receptor have been identified and optimized ultimately leading to the clinical candidate PF-06372865 (compound **34**).³⁶ During the course of these studies, multiple series and subseries were explored in order to find the desired level of functional selectivity. In order to help prioritize our design and synthesis efforts, the project team utilized a probability-based approach to focus on the direct-linked imidazopyridazine series (Series 2). This work ultimately led to the identification of two preclinical candidates, compounds **34** and **46**. Although both compounds had the desired pharmacological and pharmacokinetic profiles, safety findings in the dog with compound **46** prevented further development and therefore compound **34** was ultimately progressed to clinical studies³⁶ and provides an opportunity to further study the benefits of subtype-selective GABA_A PAMs in the clinic.

CHEMICAL METHODS

Compound purity for final, tested compounds was determined by HPLC and/or LCMS and unless otherwise noted was > 95%.

General. Starting materials and other reagents were purchased from commercial suppliers and were used without further purification unless otherwise indicated. All reactions were performed under a positive pressure of nitrogen, argon or with a drying tube at ambient temperature (unless otherwise stated) in anhydrous solvents, unless otherwise indicated. Analytical thin-layer chromatography (TLC) was performed on glass-backed silica gel 60_F 254 plates (Analtech (0.25 mm)) and eluted with the appropriate solvent ratios (v/v). The reactions were assayed by high performance liquid chromatography (HPLC) or TLC and terminated as judged by the consumption of starting material. The TLC plates were visualized by phosphomolybdic acid stain or iodine stain. Microwave assisted reactions were run in a Biotage initiator. ^1H NMR spectra were recorded on a Bruker instrument operating at 400 MHz unless otherwise indicated. ^1H NMR spectra are obtained as DMSO- d_6 or CDCl_3 solutions as indicated (reported in ppm), using chloroform as the reference standard (7.25 ppm) or DMSO- d_6 (2.50 ppm). Other NMR solvents were used as needed. When peak multiplicities are reported, the following abbreviations are used: s = singlet, d = doublet, t = triplet, m = multiplet, br = broadened, dd = doublet of doublets, dt = doublet of triplets. Coupling

constants, when given, are reported in hertz. Mass spectral data were obtained using Waters ZQ ESCI or Applied Biosystem's API-2000 using either electrospray ionisation (ESI) or atmospheric pressure chemical ionisation (APCI). High resolution mass measurements were carried out on an Agilent TOF 6200 series with ESI. Where reverse phase column chromatography has been used, either acidic or basic conditions were employed using a Biotage SNAP KP-C18 silica cartridge: **Acidic conditions:** between 0 and 100% of acetonitrile (with 0.1% formic acid) in water (with 0.1% formic acid). **Basic conditions:** between 0 and 100% of acetonitrile (with 0.1% ammonia) in water (with 0.1% ammonia, 33% aqueous ammonia used).

LCMS Conditions:

System 1: A: water, B: acetonitrile, C: 0.05% formic acid in acetonitrile, Column: XBridge analytical column C18 5µm 4.6x50mm (part no. 186003113), Gradient: 95-5% A with 5% C over 3.5 min, 1.0 min hold, 0.1 min re-equilibration, 2.0 mL/min flow rate, Temperature: 25°C

System 2: A: 10 mmol ammonium formate in water, B: acetonitrile, Column: XBridge analytical column C18 5µm 4.6x50mm (part no. 186003113), Gradient: 95-0% A over 3.5 min, 1.0 min hold, 0.1 min re-equilibration, 2.0 mL/min flow rate, Temperature: 25°C

System 6: A: water, B: acetonitrile, C: 10 mmol ammonia formate in water, Column: XBridge analytical column C18 5µm 4.6x50mm (part no. 186003113), Gradient: 95-5% A with 5% C over 3.5 min, 1.0 min hold, 0.1 min re-equilibration, 2.0 mL/min flow rate, Temperature: 25°C

System 8: A: 5mM ammonium acetate in water, B: acetonitrile, Column: Unison US C18 phase 50 x 4.6mm with 5 micron particle size, Gradient: 98% A for 0.01 min, 90% A for 0.5 min, 90-50% A over 3.5 min, 50-90% A for 1.5 min, 2.5 min hold, returned to 98% A in 0.5 min, 1 mL/min flow rate, UV: 238nm DAD, Temperature: 25°C

System 11: A: 0.5% formic acid in water, B: acetonitrile, Column: Gemini NX C18 phase 50 x 4.6mm with 3 µm particle size, Gradient: 95% A for 0.5 min, 50% A over 3.0 min, 10% A over 1.0 min, 3.0 min hold, returned to 95% A in 1.0 min, 1 mL/min flow rate, Temperature: 25°C

System 12: A: water, B: acetonitrile, C: 0.05% formic acid in acetonitrile, Column: Phenomenex Kinetex EVO C18 5µm, 150 x 4.60mm column, Gradient: 91-0% A with 5% C over 13 min, 9.5. min hold, 0.1 min re-equilibration, 1.0 mL/min flow rate, Temperature: 25°C

Compound Synthesis:

7-Ethyl-4-(4-fluorophenyl)-7H-imidazo[4,5-c]pyridazine (1)³³ To a solution of 4-chloro-7-ethyl-7H-imidazo[4,5-c]pyridazine (51,

9.6 g, 52.4 mmol) in dioxane was added 4-fluorobenzeneboronic acid (8.8 g, 63 mmol) and an aq. solution of Na₂CO₃ (1M, 260 mL, 262 mmol) at rt. The reaction mixture was degassed and purged with nitrogen gas 3 times. Pd(PPh₃)₄ (1.2 g, 1.0 mmol) was added and the mixture was heated to reflux for 4 h. The organic solvent was removed *in vacuo* and the resulting aqueous mixture was filtered. The filter cake was dried under vacuum to afford 1 as a yellow solid (7 g, 55%). LCMS (system 1) Rt 2.24 min, 98% purity (210-450 nm); HRMS-ESI (*m/z*): [M+H]⁺ calcd for C₁₃H₁₂FN₄, 243.1046; found, 243.1042; ¹H NMR (400 MHz, CDCl₃) δ 9.35 (s, 1H), 8.28 (s, 1H), 8.26 - 8.20 (m, 2H), 7.31 - 7.24 (m, 2H), 4.58 (q, *J* = 7.3 Hz, 2H), 1.69 (t, *J* = 7.3 Hz, 3H).

7-Ethyl-4-(4-fluoro-3-(pyridin-3-yl)phenyl)-7H-imidazo[4,5-c]pyridazine (5) To a solution of 4-(3-chloro-4-fluorophenyl)-7-ethyl-7H-imidazo[4,5-c]pyridazine (54, 0.3 g, 65% purity, 0.7 mmol) and pyridin-3-ylboronic acid (0.17 g, 1.4 mmol) in 1,4-dioxane (5 mL) was added Cs₂CO₃ (0.46 g, 1.4 mmol) and water (1 mL). The resulting solution was degassed for 20 min. After adding Pd(dppf)Cl₂ (46 mg, 0.07 mmol), the reaction mixture was heated at 100 °C for 2 h. After cooling to rt, it was diluted with ethyl acetate, filtered through a pad of silica/MgSO₄, and concentrated *in vacuo*. The crude mixture was purified by column chromatography (100% ethyl acetate to 10% MeOH in ethyl acetate) to afford 5 (84 mg) as an off-white

solid. LCMS (system 2), Rt 2.46 min, 98% purity (210-450 nm); HRMS-ESI (m/z): $[M+H]^+$ calcd for $C_{18}H_{15}FN_5$, 320.1311; found, 320.1319; 1H NMR (400 MHz, $CDCl_3$) δ 9.39 (s, 1H), 8.90 (s, 1H), 8.66 (dd, J = 4.8, 1.7 Hz, 1H), 8.41 (dd, J = 7.3, 2.3 Hz, 1H), 8.28 (s, 1H), 8.23 (ddd, J = 8.5, 4.6, 2.4 Hz, 1H), 7.97 (dd, J = 7.8, 2.0 Hz, 1H), 7.42 (dt, J = 10.1, 6.9 Hz, 2H), 4.59 (q, J = 7.3 Hz, 2H), 1.70 (t, J = 7.3 Hz, 3H).

5-(5-(7-Ethyl-7H-imidazo[4,5-c]pyridazin-4-yl)-2-fluorophenoxy)pyrimidine-2-carbonitrile (13) A solution of 5-(7-ethyl-7H-imidazo[4,5-c]pyridazin-4-yl)-2-fluorophenol (57, 50 mg, 0.19 mmol), 5-bromopyrimidine-2-carbonitrile (71 mg, 0.39 mmol), and K_2CO_3 (54 mg, 0.39 mmol) in DMF (2 mL) was heated at 50 °C for 2 h. The resulting crude mixture was purified by library auto-purification system. LCMS (system 6) Rt 2.34 min, 96% purity (210-450 nm); HRMS-ESI (m/z): $[M+H]^+$ calcd for $C_{18}H_{13}FN_7O$, 362.1166; found, 362.1171.

8-Ethyl-4-(4'-(ethylsulfonyl)-6-fluorobiphenyl-3-yl)pyrazolo[5,1-c][1,2,4]triazine (28) To a stirred solution of 4-ethyl-1H-pyrazol-5-amine (195 mg, 1.76 mmol) in water (2.8 mL) was added conc. HCl (1.4 mL) at 0 °C, followed by aq. solution of $NaNO_2$ (121 mg, 1.76 mmol) dropwise. The ice bath was removed, and the resulting mixture was stirred at rt for 45 min. Once it was re-cooled to 0 °C, saturated aq. solution of Na_2CO_3 was added carefully to basicify the solution. A solution of (2-(4'-

(Ethylsulfonyl)-6-fluorobiphenyl-3-yl)-2-oxoethyl)triphenylphosphonium ylide (91, 1.0 g, 1.76 mmol) in DCM (50 mL) was added at 0 °C. The resulting mixture was stirred at 0 °C for 2 h before quenching with sat. aq. Na₂S₂O₃ solution. Organic layer was separated, and the aq. layer was further extracted with DCM (10 mL). The combined organic layer were dried over Na₂SO₄, filtered, and concentrated. The resulting crude material was purified by column chromatography (30% EtOAc in hexanes) to afford 28 (128 mg, 18%). LCMS (system 8), Rt 3.74 min, >95% purity (238 nm); HRMS-ESI (*m/z*): HRMS-ESI (*m/z*): [M+H]⁺ calcd for C₂₁H₂₀FN₄O₂S, 411.1291; found, 411.1290; ¹H NMR (400MHz, CDCl₃) δ 8.86 (s, 1H), 8.44 – 8.42 (m, 1H), 8.21 – 8.26 (m, 1H), 8.16 (s, 1H), 8.02 (d, *J* = 8.2 Hz, 2H), 7.82 (d, *J* = 7.8 Hz, 2H), 7.45 (t, *J* = 9.1 Hz, 1H), 3.20 – 3.13 (m, 4H), 1.47 (t, *J* = 7.6 Hz, 3H), 1.33 (t, *J* = 7.4 Hz, 3H).

7-Ethyl-4-[4'-(ethylsulfonyl)-6-fluoro-2'-methoxybiphenyl-3-yl]-7H-imidazo[4,5-*c*]pyridazine (34)³³ A solution of 7-ethyl-4-(4-fluoro-3-iodophenyl)-7H-imidazo[4,5-*c*]pyridazine (53, 2 g, 6.2 mmol), B₂Pin₂ (2.37g, 9.3 mmol), KOAc (1.2g, 12.5 mmol) in 1,4-dioxane (40 mL) was added PdCl₂(dppf) (0.5 g, 0.62 mmol). The resulting mixture was heated for 2.5 h at 100 °C. The reaction mixture was allowed to cool and then 2M Na₂CO₃ was added followed by 1-Bromo-4-(ethylsulfonyl)-2-methoxybenzene (61, 2.0 g, 7.2 mmol) and PdCl₂(dppf) (0.5 g, 0.62 mmol). The reaction was run at

100 °C for 2 h. The reaction mixture was filtered, partitioned between ethyl acetate (800 mL) and water (200 mL). Organic layer was separated, and aq. layer was further extracted with ethyl acetate (3 × 1 L). The combined organic layers were concentrated, purified by column chromatography (50 - 90% Ethyl acetate with DCM) to afford 2.2 g of off-white solid 34 (80%). HPLC (system 11) Rt 4.64 min, 96% purity (220 nm); HRMS-ESI (*m/z*): [M+H]⁺ calcd for for C₂₂H₂₂FN₄O₃S, 441.1397; found, 441.1403; ¹H NMR (400MHz, CDCl₃) δ 9.35 (s, 1H), 8.27-8.29 (m, 1H), 8.26 (s, 1H), 8.21 (dd, *J* = 6.8, 2.0 Hz, 1H), 7.54-7.60 (m, 2H), 7.50 (s, 1H), 7.35 (t, *J* = 9.0 Hz, 1H), 4.58 (q, *J* = 7.3 Hz, 2H), 3.90 (s, 3H), 3.18 (q, *J* = 7.4 Hz, 2H), 1.68 (t, *J* = 7.4 Hz, 3H), 1.36 (t, *J* = 7.4 Hz, 3H).

5-[5-(7-Ethyl-7*H*-imidazo[4,5-*I*]pyridazin-4-yl)-2-fluorophenyl]-6-methoxy-2-methyl-2,3-dihydro-1*H*-isoindol-1-one (46) To a solution of 6-methoxy-2-methyl-5-(4,4,5,5-tetramethyl-1,3,2-dioxaborolan-2-yl)isoindolin-1-one (67, 3.00 g, 9.90 mmol) and 4-(3-bromo-4-fluorophenyl)-7-ethyl-7*H*-imidazo[4,5-*c*]pyridazine (53, see scheme 8, 2.86 g, 8.91 mmol) in 1,4-dioxane (180 mL) and water (50 mL) at room temperature was added potassium carbonate (3.4 g, 24.7 mmol). The solution was degassed with nitrogen for 30 minutes before tetrakis(triphenylphosphine)palladium(0) (0.57 g, 4.95 mmol) was added and the reaction heated to 110 °C. After 62 hours the

reaction was cooled to room temperature and diluted with ethyl acetate (150 mL). The organic layer was washed with ammonium chloride solution (2 x 150 mL), brine (150 mL), dried over sodium sulfate, filtered and concentrated *in vacuo*. The crude residue was dissolved in dichloromethane (15 mL) and purified through an SCX column eluting initially with DCM:MeOH 150 mL:400 mL followed by aqueous ammonium hydroxide in methanol (0.880 M; 200 mL) to afford a yellow solid. The solid was triturated in methanol (50 mL), filtered, washed with methanol (150 mL) and air dried to afford a colourless solid (1.30 g). The mother liquor was concentrated *in vacuo*, triturated in methanol (20 mL), filtered, washed with methanol (50 mL) and air dried to afford a colourless solid (0.21 g). The solids were combined to afford 46 (1.51 g, 37%). LCMS (system 12) Rt 12.01 min, 99% purity (210-450 nm); HRMS-ESI (m/z): $[M+H]^+$ calcd for $C_{23}H_{21}FN_5O_2$, 418.1679; found, 418.1679; 1H NMR (400 MHz, $CDCl_3$) δ 9.41 (s, 1H), 8.37 (s, 1H), 8.33 (ddd, J = 8.6, 4.8, 2.4 Hz, 1H), 8.23 (dd, J = 6.8, 2.4 Hz, 1H), 7.47 (s, 1H), 7.42 (s, 1H), 7.37 (t, J = 9.0 Hz, 1H), 4.59 (q, J = 7.3 Hz, 2H), 4.39 (s, 2H), 3.89 (s, 3H), 3.24 (s, 3H), 1.70 (t, J = 7.3 Hz, 3H).

5-Chloro-N3-ethylpyridazine-3,4-diamine (50) A mixture of 3,5-(dichloropyridazin-4-yl)amine (49, 15 g, 92 mmol) and anhydrous ethylamine (50 mL) was heated to 120 °C for 48 hours in a sealed tube. The reaction mixture was cooled to room temperature, and

then added to a mixture of water (500 mL) and EtOAc (50 mL). The resulting precipitate was separated by filtration and the filter cake was washed with MTBE, and dried under vacuum to afford 50 as off-white solid in 51% yield, 8.1 g. LCMS (m/z): [M+H]⁺ 173.1; ¹H NMR (500 MHz, DMSO-d₆) δ 8.11 (s, 1 H) 6.05 - 6.20 (m, 3 H) 3.41 (qd, *J* = 7.20, 5.0 Hz, 2 H) 1.20 (t, *J* = 7.2 Hz, 3 H).

4-Chloro-7-ethyl-7H-imidazo[4,5-c]pyridazine (51) A mixture of 5-Chloro-N³-ethylpyridazine-3,4-diamine (50, 10.0 g, 58 mmol) and triethylorthoformate (60 mL) were heated to reflux for 4 hours. The reaction mixture was concentrated *in vacuo* and the residue was dissolved in EtOAc (50 mL) and filtered. The filter cake was washed with EtOAc and then the organic layers were washed with saturated brine solution, dried over Na₂SO₄ and concentrated *in vacuo* to afford 51 as a yellow solid in 45% yield, 4.8g. LCMS (m/z): [M+H]⁺ 183.1; ¹H NMR (500 MHz, DMSO-d₆) δ 9.25 (s, 1 H) 8.93 (s, 1 H) 4.49 (q, *J* = 7.2 Hz, 2 H) 1.54 (t, *J* = 7.2 Hz, 3 H).

4-(3-Bromo-4-fluorophenyl)-7-ethyl-7H-imidazo[4,5-c]pyridazine (53)³³ Concentrated sulphuric acid (66 g, 0.67 mol) was carefully added to 7-ethyl-4-(4-fluorophenyl)-7H-imidazo[4,5-c]pyridazine (1, 2.3 g, 9.5 mmol) surrounded by an ice bath, and the resultant reaction mixture was gently stirred at room temperature until a homogeneous solution was observed. To this solution was added 1,3-dibromo-5,5-dimethylhydantoin (2.7 g, 9.5

mmol) portion-wise, and stirring was continued at 0 °C for 2 hours. The reaction mixture was poured carefully into aqueous sodium bisulphite (200 mL), and then basified with an aqueous sodium hydroxide solution (2 M) to pH = 8 keeping the temperature below 20 °C. EtOAc (50 mL) was added and the layers were separated. The aqueous layer was extracted with EtOAc (2 x 50 mL). The combined organic phases were washed with saturated brine solution, dried over Na₂SO₄ and concentrated *in vacuo*. The residue was purified by silica gel column chromatography eluting with petroleum ether:CH₂Cl₂ 1:1 followed by trituration with EtOAc to afford 53 as a white solid in 41% yield, 1.25g. LCMS (m/z): [M+H]⁺ 348; ¹H NMR (400 MHz, CDCl₃) δ 9.32 (s, 1H), 8.44-8.50 (m, 1H), 8.31 (s, 1H), 8.16-8.25 (m, 1H), 7.26-7.34 (m, 1H), 4.58 (q, *J* = 7.3 Hz, 2H), 1.70 (t, *J* = 7.3 Hz, 3H).

4-(3-Chloro-4-fluorophenyl)-7-ethyl-7H-imidazo[4,5-c]pyridazine (54) To a solution of 4-chloro-7-ethyl-7H-imidazo[4,5-c]pyridazine (51, 0.5 g, 2.7 mmol) and 3-chloro-4-fluorophenylboronic acid (0.59 g, 4.1 mmol) in 1,4-dioxane (7.5 mL) was added Cs₂CO₃ (1.8 g, 5.5 mmol) and water (1.5 mL). The resulting solution was degassed for 20 min. Pd(PPh₃)₄ (0.32 g, 0.27 mmol) was added. The mixture was heated at 100 °C for 8 h. The reaction mixture was diluted with ethyl acetate (30 mL), and filtered through a pad of silica and magnesium sulfate. The solvent was removed *in vacuo* to give a 2:1 mixture (by ¹H NMR

integration) of 54 and triphenylphosphine oxide (0.91 g), which was used directly in the next step. LCMS (m/z): [M+H]⁺ 277.1; ¹H NMR (400 MHz, CDCl₃) δ 9.33 (s, 1H), 8.36 (d, 1H), 8.30 (s, 1H), 8.17 – 8.11 (m, 1H), 7.34 (t, 1H), 4.60 (q, 2H), 1.72 (t, 3H).

5-(7-Ethyl-7H-imidazo[4,5-c]pyridazin-4-yl)-2-fluorophenol (57)

Aluminum chloride (4.53 g, 34.03 mmol) was added to a suspension of 7-ethyl-4-(4-fluoro-3-methoxyphenyl)-7H-imidazo[4,5-c]pyridazine (58, 3.1 g, 11.34 mmol) in toluene (100 ml) and heated to reflux for 16 h. After completion of reaction by TLC, the reaction mixture was diluted with ice cold water (500 ml) at 0 °C and extracted with ethyl acetate (2 X 300 ml). The organic layer was dried over Na₂SO₄ and concentrated to get 1.8 g of crude compound. The crude product was triturated with EtOAc and pentane (1:1, 30 ml), filtered and dried to afford 1.5 g of 57 (51%). LCMS (m/z): [M+H]⁺ 259.0; ¹H NMR (500 MHz, DMSO-d₆) δ 10.24 (s, 1H), 9.41 (s, 1H), 8.87 (s, 1H), 8.13 (dd, J = 8.7, 2.3 Hz, 1H), 7.79 (ddd, J = 8.5, 4.3, 2.3 Hz, 1H), 7.35 (dd, J = 11.2, 8.5 Hz, 1H), 4.50 (q, J = 7.3 Hz, 2H), 1.56 (t, J = 7.3 Hz, 3H).

7-Ethyl-4-(4-fluoro-3-methoxyphenyl)-7H-imidazo[4,5-c]pyridazine (58) To a de-gassed solution of 4-chloro-7-ethyl-7H-imidazo[4,5-c]pyridazine (51), 4 g, 21.90 mmol), 3-fluoro-4-methoxyphenylboronic acid (4 g, 24.09 mmol) and 2M Na₂CO₃ in 1,4-dioxane (100 ml) was added Pd(dppf)Cl₂ (893 mg, 1.09 mmol).

It was heated to reflux for 16 h. After completion of reaction by TLC, the reaction mixture was filtered through a pad of celite, washed with EtOAc (200 ml) and the filtrate was washed with water (100 ml). The organic layer was dried over Na₂SO₄ and concentrated. The crude product was purified by column chromatography using 20% EtOAc in pet ether as eluent to afford 58 (2.5 g, 42%). LCMS (m/z): [M+H]⁺ 273.1; ¹H NMR (500 MHz, DMSO-d₆) δ 9.57 (s, 1H), 8.88 (s, 1H), 8.21 (dd, *J* = 8.4, 2.2 Hz, 1H), 8.06 (ddd, *J* = 8.5, 4.4, 2.1 Hz, 1H), 7.44 (dd, *J* = 11.4, 8.5 Hz, 1H), 4.51 (q, *J* = 7.3 Hz, 2H), 3.98 (s, 3H), 1.56 (t, *J* = 7.3 Hz, 3H).

1-Bromo-4-(ethylsulfonyl)-2-fluorobenzene (60)³³ To solution of 4-bromo-3-fluorobenzene-1-sulfonyl chloride (50 g, 0.184 mol) in THF (800 mL) at 0°C was added hydrazine monohydrate (40-50%, 41.26 g, 0.64 mol) dropwise over 45 minutes. The reaction was stirred for 4 hours at room temperature and then the solvent was removed under reduced pressure to low volume. Heptane (100 mL) was added and the solid was filtered and washed several times with heptanes. The resulting solid was dissolved in ethanol (800 mL). Sodium acetate (90.56 g, 1.10 mol) and ethyl iodide (143.49 g, 0.92 mol) were added and the reaction heated to reflux for 18 hours. The reaction was allowed to cool to room temperature, the solvent was removed under reduced pressure to 30% of the initial volume. The reaction mixture was diluted with water (500 mL) and

1
2
3 extracted with CH_2Cl_2 (3x 250 mL). The combined organic layers
4
5 were washed with brine (2x300 mL), dried over Na_2SO_4 , filtered
6
7 and reduced to dryness to give a yellow oil. The crude was
8
9 absorbed onto silica and purified (using silica gel column
10
11 chromatography eluting with cyclohexane/EtOAc 8/2 to give 60 as
12
13 yellow solid in 64% yield, 31.70 g. LCMS (m/z): no ionization; ^1H
14
15 NMR (400 MHz, $\text{DMSO}-d_6$) δ 1.10 (t, $J = 7.3$ Hz, 3H), 3.39 (q, $J =$
16
17 7.3 Hz, 2H), 7.67 (dd, $J = 8.3, 1.2$ Hz, 1H), 7.89 (dd, $J = 8.2,$
18
19 1.8 Hz, 1H), 7.89 (dd, $J = 7.9, 7.1$ Hz, 1H).

20
21
22
23 **1-Bromo-4-(ethylsulfonyl)-2-methoxybenzene (61)**³³ In a sealed
24
25 vessel, 1-bromo-4-(ethylsulfonyl)-2-fluorobenzene (60, 34.9 g,
26
27 0.13 mol) was dissolved in MeOH (400 mL) and sodium methoxide
28
29 (35.3 g, 0.65 mol) was added. The reaction was heated at 100 °C
30
31 for 12 hours and then allowed to cool to room temperature. The
32
33 reaction mixture was diluted with water (750 mL) and the aqueous
34
35 layer was extracted with CH_2Cl_2 (2 x 250 mL). The combined
36
37 organic layers were washed with brine (300 mL), dried over
38
39 Na_2SO_4 , filtered and reduced to dryness to give a solid. The
40
41 crude was purified by silica gel column chromatography eluting
42
43 with cyclohexane/EtOAc gradient from 95/5 to 8/2 to afford 61
44
45 as colourless solid in 75% yield, 27.3 g. LCMS (m/z): no
46
47 ionization; ^1H NMR (400 MHz, CDCl_3) δ 1.29 (t, $J = 7.5$ Hz, 3H),
48
49 3.12 (q, $J = 7.4$ Hz, 2H), 3.97 (s, 3H), 7.35-7.38 (m, 2H), 7.74
50
51 (d, $J = 8.7$ Hz, 1H).

Methyl 2-bromo-4-chloro-5-methoxybenzoate (63) To a suspension of methyl 4-chloro-3-methoxybenzoate (62, 155 g, 773 mmol) in AcOH (775 mL) and water (775 mL) was added bromine (64 mL, 1.2 mol) dropwise over 10 minutes. The reaction was heated to 60°C for 18 hour. The reaction was cooled to room temperature, and the resulting precipitate filtered, washed with water (3 x 150 mL) and dried. The resulting solid was slurried in hot (60°C) ethanol and filtered to afford the title compound (63) as a slightly orange solid (327.3 g, 76%). The filtrate was concentrated until a slurry formed and then filtered to afford additional product (22.7 g, 11%) LCMS (m/z): no ionization; ¹H NMR (400 MHz, CDCl₃) δ 7.66 (s, 1H), 7.38 (s, 1H), 3.94 (s, 3H), 3.93 (s, 3H).

Methyl 4-chloro-2-cyano-5-methoxybenzoate (64) Methyl 2-bromo-4-chloro-5-methoxybenzoate (63, 96 g, 340 mmol) and copper cyanide (33.8 g, 378 mmol) were dissolved in DMF (400 mL) and heated to 150°C for 1.5 hours. Upon cooling a precipitate formed, which was filtered and washed with DMF, concentrated with reduced pressure with heating (70°C). The resulting mixture was diluted with DCM (1.5 L), washed with sat. NH₄Cl solution (2 x 750 mL). The combined aqueous layer was back-extracted with DCM (250 mL). The combined organic layers were dried over MgSO₄, filtered, concentrated to afford 64.6 g (83%) of 64 as a

greenish gray solid. ^1H NMR (400 MHz, CDCl_3) δ 7.77 (s, 1H), 7.64 (s, 1H), 4.01 (s, 6H).

5-Chloro-6-methoxyisoindolin-1-one (65) Methyl 4-chloro-2-cyano-5-methoxybenzoate (64, 180 mg, 0.798 mmol) was dissolved in MeOH (20 mL) and EtOAc (5 mL) by gentle heating. Sat. aqueous ammonia (0.5 mL) was added and the reaction hydrogenated over Raney Nickel (150 mg) at 45 psi for 5 hours. The reaction was filtered through celite and concentrated *in vacuo*. The residue was purified using silica gel column chromatography eluting with 0.5-2% MeOH in DCM to afford the title compound (65) as an off white powder (105 mg, 67%), which contained approximately 10% dechlorination side product. LCMS (m/z) $[\text{M}+\text{H}]^+ = 198$; ^1H NMR (400 MHz, CDCl_3) δ 7.50 (s, 1H), 6.46 (br s, 1H), 4.39 (s, 2H), 3.97 (s, 3H).

5-Chloro-6-methoxy-2-methylisoindol-1-one (66) To a suspension of 5-chloro-6-methoxyisoindolin-1-one (65, 105 mg, 0.53 mmol) in THF (3 mL) at 0 °C was added NaH (60% dispersion in oil, 22 mg, 0.55 mmol) and the reaction was stirred at this temperature for 10 minutes followed by room temperature for 10 minutes. The reaction was cooled back to 0°C, iodomethane (38 μL , 0.61 mmol) was added and the reaction was stirred warming to room temperature for 18 hours. The reaction was quenched by the addition of water (few drops) and partitioned between EtOAc (40 mL) and aqueous ammonium chloride solution (30 mL). The organic

layer was collected, dried over Na_2SO_4 and concentrated *in vacuo* to afford the title compound as a beige powder (66, 102 mg, 91%). LCMS (m/z) $[\text{M}+\text{H}]^+ = 212$; ^1H NMR (400 MHz, CDCl_3) δ 7.45 (s, 1H), 7.37 (s, 1H), 4.30 (s, 2H), 3.96 (s, 3H), 3.19 (s, 3H)

6-methoxy-2-methyl-5-(4,4,5,5-tetramethyl-1,3,2-dioxaborolan-2-yl)isoindolin-1-one (67) A solution of 5-chloro-6-methoxy-2-methylisoindolin-1-one (66, 90 mg, 0.43 mmol), 4,4,4',4',5,5,5',5'-octamethyl-2,2'-bi(1,3,2-dioxaborolane) (140 mg, 0.55 mmol) and potassium acetate (80 mg, 0.81 mmol) in 1,4-dioxane (1.5 mL) at room temperature was degassed with nitrogen. After 1 hour tricyclohexylphosphine (27 mg, 0.096 mmol) and tris(dibenzylideneacetone)dipalladium(0) (18 mg, 0.020 mmol) were sequentially added and the reaction heated to 110 °C. After 18 hours the reaction was cooled to room temperature and the solution filtered through celite, washed with ethyl acetate (3 x 50 mL) and concentrated *in vacuo*. The residue was purified using silica gel column chromatography eluting with 20-100% ethyl acetate in heptanes followed by tritiated in 50% EtOAc in heptanes to afford the title compound as a colourless solid (67, 120 mg, 94%). LCMS (m/z) $[\text{M}+\text{H}]^+ = 222$ (boronic acid); ^1H NMR (400 MHz, CDCl_3): δ ppm 7.69 (s, 1H), 7.29 (s, 1H), 4.29 (s, 2H), 3.89 (s, 3H), 3.20 (s, 3H), 1.37 (s, 12H).

5-Chloro-N3-isopropylpyridazine-3,4-diamine (68) Acetic acid (2.47 mL, 42.7 mmol) was added dropwise to a mixture of 3,5-

dichloropyridazin-4-amine (49, 1000 mg, 6.098 mmol) and isopropylamine (7.27 mL, 85.4 mmol) cooled to 0 °C. The resulting solid/suspension was heated under microwave irradiation at 105 °C for 5 hours. The reaction mixture was dissolved in minimum amount of MeOH and purified by silica gel column chromatography eluting with 10% MeOH in DCM to provide 68 as a slightly brownish solid in 74% yield, 2.52 g. LCMS (m/z): [M+H]⁺ 187; ¹H NMR (400 MHz, CDCl₃): δ 8.29 (s, 1H). 5.06 (s, 2H), 4.91 (d, *J* = 7.1 Hz, 1H), 4.43 - 4.30 (m, 1H), 1.22-1.25 (m, 6H).

Biological Methods

All experiments performed in the United Kingdom were conducted in accordance with the Home Office Animals (Scientific Procedures) Act (1986) and were subject to local ethical review. All procedures involving animals in the United States were conducted with approval of the Pfizer and were compliant with US National Research Council's Guide for the Care and Use of Laboratory Animals, the US Public Health Service's Policy on Humane Care and Use of Laboratory Animals, and Guide for the Care and Use of Laboratory Animals.

α₂ Ki and α₁/α₂ PAM/functional values were measured as described here.³³⁻³⁵

Other GABA_A subtype (α₁, α₅, etc) Ki and functional values, and Occ₅₀ values were measured as described here.³⁶

ASSOCIATED CONTENT

Supporting Information

The Supporting Information is available free of charge on the ACS Publications website.

Characterization details (1H NMR spectra and HPLC/LCMS traces) for all final compounds, synthetic details for all remaining compounds not described above and further details on in vivo studies for Compounds **34** and **46** (PDF)

Molecule formula strings (CSV)

Corresponding Author

*Phone +44 (0)1304 644 533, email: robert.owen@pfizer.com

Present Addresses

For A.P.: DMPK, Oncology, IMED Biotech Unit, AstraZeneca, Cambridge, United Kingdom.

For D.P.: Curadev Pharma Ltd., Discovery Park House, Ramsgate Road, Sandwich, Kent, CT13 9ND, United Kingdom.

For S.A.N.: GSK Medicines Research Centre, Gunnels Wood Road, Stevenage, Hertfordshire, SG1 2NY, United Kingdom.

For R.R.: Axovant Sciences, Inc., 324 Blackwell St, Suite 1220, Durham, NC 27701, USA.

For E.M-C: Drug Safety and Metabolism, IMED Biotech Unit,
AstraZeneca, Cambridge, United Kingdom

Author Contributions

The manuscript was written through contributions of all authors.
All authors have given approval to the final version of the
manuscript.

Notes

All procedures performed on animals were in accordance with
regulations and established guidelines and were reviewed and
approved by an Institutional Animal Care and Use Committee or
through an ethical review process.

ACKNOWLEDGMENT

The authors wish to thank Philip Miliken for help collating the
safety-related data. They would also like to thank Manish
Bangerjee, Subhasis Roy, Revun Sandeep Kumar and Chaitali Mondal
of TCG Lifesciences, India for performing the CCI studies.

ABBREVIATIONS

ADME, absorption distribution metabolism excretion; AUC, area
under curve; Boc, tert-butyloxycarbonyl; Clint, intrinsic
clearance; Cmax, maximum concentration; Clp, plasma clearance;
Clu, unbound clearance; CYP, cytochrome P450; DDI, drug-drug
interaction; DLM, dog liver microsomes; DMB, dimethoxy benzyl; F,

bioavailability; *Fu*, fraction unbound; *HBA*, H-bond acceptor; *HBD*, H-bond donor; *hep*, hepatocytes; *HET*, heterocycle; *HLM*, human liver microsomes; *IV*, intravenous; *LHS*, left-hand side; *LipE*, lipophilic efficiency; *MDCK-MDR1*, Madin-Darby canine kidney, multidrugresistance; *OATP*, organic anion-transporting polypeptide; *Papp*, apparent permeability; *PK*, pharmacokinetics; *PPB*, plasma protein binding; *RHS*, right-hand side; *RLM*, rat liver microsomes; *RRCK*, Ralph Russ canine kidney; *SAR*, structure-activity relationship; *T_{1/2}*, plasma half-life; *T_{max}*, time at maximum plasma concentration; *TPSA*, topological polar surface area; *V_{ss}*, volume of distribution (steady state); *GABA_A*, γ -amino butyric acid-A; *CNS*, central nervous system; *Occ₅₀*, dose required to produce 50% occupancy; *THLE*, T-antigen-immortalized Human Liver Epithelial

REFERENCES

1. D'Hulst, C.; Atack, J. R.; Kooy, R. F., The complexity of the GABAA receptor shapes unique pharmacological profiles. *Drug Discovery Today* **2009**, *14* (17/18), 866-875.
2. McKernan, R. M.; Whiting, P. J., Which GABAA-receptor subtypes really occur in the brain? *Trends Neurosci* **1996**, *19* (4), 139-143.
3. Sieghart, W.; Sperk, G., Subunit composition, distribution and function of GABAA receptor subtypes. *Curr. Top. Med. Chem. (Hilversum, Neth.)* **2002**, *2* (8), 795-816.
4. Whiting, P. J.; Bonnert, T. P.; McKernan, R. M.; Farrar, S.; Le Bourdelles, B.; Heavens, R. P.; Smith, D. W.; Hewson, L.; Rigby, M. R.; Sirinathsinghji, D. J. S.; Thompson, S. A.; Wafford, K. A., Molecular and functional diversity of the expanding GABA-A receptor gene family. *Ann. N. Y. Acad. Sci.* **1999**, *868* (Molecular and Functional Diversity of Ion Channels and Receptors), 645-653.
5. Munro, G.; Hansen, R. R.; Mirza, N. R., GABAA receptor modulation: Potential to deliver novel pain medicines? *Eur. J. Pharmacol.* **2013**, *716* (1-3), 17-23.

6. Rudolph, U.; Knoflach, F., Beyond classical benzodiazepines: novel therapeutic potential of GABAA receptor subtypes. *Nat. Rev. Drug Discovery* **2011**, *10* (9), 685-697.

7. Zeilhofer, H. U.; Moehler, H.; Di Lio, A., GABAergic analgesia: new insights from mutant mice and subtype-selective agonists. *Trends Pharmacol. Sci.* **2009**, *30* (8), 397-402.

8. Atack, J. R., GABAA receptor subtype-selective modulators. I. $\alpha 2/\alpha 3$ -selective agonists as non-sedating anxiolytics. *Curr. Top. Med. Chem. (Sharjah, United Arab Emirates)* **2011**, *11* (9), 1176-1202.

9. McKernan, R. M.; Rosahl, T. W.; Reynolds, D. S.; Sur, C.; Wafford, K. A.; Atack, J. R.; Farrar, S.; Myers, J.; Cook, G.; Ferris, P.; Garrett, L.; Bristow, L.; Marshall, G.; Macaulay, A.; Brown, N.; Howell, O.; Moore, K. W.; Carling, R. W.; Street, L. J.; Castro, J. L.; Ragan, C. I.; Dawson, G. R.; Whiting, P. J., Sedative but not anxiolytic properties of benzodiazepines are mediated by the GABA(A) receptor $\alpha 1$ subtype. *Nat Neurosci* **2000**, *3* (6), 587-592.

10. Knabl, J.; Witschi, R.; Hosl, K.; Reinold, H.; Zeilhofer, U. B.; Ahmadi, S.; Brockhaus, J.; Sergejeva, M.; Hess, A.; Brune, K.; Fritschy, J. M.; Rudolph, U.; Mohler, H.; Zeilhofer,

H. U., Reversal of pathological pain through specific spinal GABAA receptor subtypes. *Nature* **2008**, 451 (7176), 330-334.

11. Dias, R.; Sheppard, W. F.; Fradley, R. L.; Garrett, E. M.; Stanley, J. L.; Tye, S. J.; Goodacre, S.; Lincoln, R. J.; Cook, S. M.; Conley, R.; Hallett, D.; Humphries, A. C.; Thompson, S. A.; Wafford, K. A.; Street, L. J.; Castro, J. L.; Whiting, P. J.; Rosahl, T. W.; Attack, J. R.; McKernan, R. M.; Dawson, G. R.; Reynolds, D. S., Evidence for a significant role of alpha 3-containing GABAA receptors in mediating the anxiolytic effects of benzodiazepines. *J Neurosci* **2005**, 25 (46), 10682-10688.

12. Attack, J. R.; Wafford, K. A.; Tye, S. J.; Cook, S. M.; Sohal, B.; Pike, A.; Sur, C.; Melillo, D.; Bristow, L.; Bromidge, F.; Ragan, I.; Kerby, J.; Street, L.; Carling, R.; Castro, J. L.; Whiting, P.; Dawson, G. R.; McKernan, R. M., TPA023 [7-(1,1-dimethylethyl)-6-(2-ethyl-2H-1,2,4-triazol-3-ylmethoxy)-3-(2-fluorophenyl)-1,2,4-triazolo[4,3-b]pyridazine], an agonist selective for alpha2- and alpha3-containing GABAA receptors, is a nonsedating anxiolytic in rodents and primates. *J Pharmacol Exp Ther* **2006**, 316 (1), 410-422.

13. Dawson, G. R.; Maubach, K. A.; Collinson, N.; Cobain, M.; Everitt, B. J.; MacLeod, A. M.; Choudhury, H. I.; McDonald, L. M.; Pillai, G.; Rycroft, W.; Smith, A. J.; Sternfeld, F.; Tattersall, F. D.; Wafford, K. A.; Reynolds, D. S.; Seabrook, G.

R.; Atack, J. R., An inverse agonist selective for alpha5 subunit-containing GABAA receptors enhances cognition. *J Pharmacol Exp Ther* **2006**, 316 (3), 1335-1345.

14. Fradley, R. L.; Guscott, M. R.; Bull, S.; Hallett, D. J.; Goodacre, S. C.; Wafford, K. A.; Garrett, E. M.; Newman, R. J.; O'Meara, G. F.; Whiting, P. J.; Rosahl, T. W.; Dawson, G. R.; Reynolds, D. S.; Atack, J. R., Differential contribution of GABA(A) receptor subtypes to the anticonvulsant efficacy of benzodiazepine site ligands. *J Psychopharmacol* **2007**, 21 (4), 384-391.

15. Rudolph, U.; Crestani, F.; Benke, D.; Brunig, I.; Benson, J. A.; Fritschy, J.-M.; Martin, J. R.; Bluethmann, H.; Mohler, H., Benzodiazepine actions mediated by specific γ -aminobutyric acidA receptor subtypes. *Nature (London)* **1999**, 401 (6755), 796-800.

16. Munro, G.; Lopez-Garcia, J. A.; Rivera-Arconada, I.; Erichsen, H. K.; Nielsen, E. O.; Larsen, J. S.; Ahring, P. K.; Mirza, N. R., Comparison of the novel subtype-selective GABAA receptor-positive allosteric modulator NS11394 [3'-[5-(1-hydroxy-1-methylethyl)benzoimidazol-1-yl]biphenyl-2-carbonitrile] with diazepam, zolpidem, bretazenil, and gaboxadol in rat models of inflammatory and neuropathic pain. *J. Pharmacol. Exp. Ther.* **2008**, 327 (3), 969-981.

17. Morlock, E. V.; Czajkowski, C., Different residues in the GABAA receptor benzodiazepine binding pocket mediate benzodiazepine efficacy and binding. *Mol. Pharmacol.* **2011**, *80* (1), 14-22.

18. Ain, Q. U.; Owen, R. M.; Omoto, K.; Torella, R.; Bulusu, K. C.; Pryde, D. C.; Glen, R. C.; Fuchs, J. E.; Bender, A., Analysis of differential efficacy and affinity of GABAA (alpha1/alpha2) selective modulators. *Mol Pharm* **2016**, *13* (11), 4001-4012.

19. Wager, T. T.; Hou, X.; Verhoest, P. R.; Villalobos, A., Moving beyond rules: the development of a central nervous system multiparameter optimization (CNS MPO) approach to enable alignment of druglike properties. *ACS Chem Neurosci* **2010**, *1* (6), 435-449.

20. Storer, R. I.; Brennan, P. E.; Brown, A. D.; Bungay, P. J.; Conlon, K. M.; Corbett, M. S.; DePianta, R. P.; Fish, P. V.; Heifetz, A.; Ho, D. K.; Jessiman, A. S.; McMurray, G.; de Oliveira, C. A.; Roberts, L. R.; Root, J. A.; Shanmugasundaram, V.; Shapiro, M. J.; Skerten, M.; Westbrook, D.; Wheeler, S.; Whitlock, G. A.; Wright, J., Multiparameter optimization in CNS drug discovery: Design of pyrimido[4,5-d]azepines as potent 5-hydroxytryptamine 2C (5-HT(2)C) receptor agonists with exquisite

functional selectivity over 5-HT(2)A and 5-HT(2)B receptors. *J Med Chem* **2014**, 57 (12), 5258-5269.

21. Hitchcock, S. A.; Pennington, L. D., Structure-brain exposure relationships. *J Med Chem* **2006**, 49 (26), 7559-7583.

22. Atack, J. R.; Wafford, K. A.; Street, L. J.; Dawson, G. R.; Tye, S.; Van Laere, K.; Bormans, G.; Sanabria-Bohorquez, S. M.; De Lepeleire, I.; de Hoon, J. N.; Van Hecken, A.; Burns, H. D.; McKernan, R. M.; Murphy, M. G.; Hargreaves, R. J., MRK-409 (MK-0343), a GABAA receptor subtype-selective partial agonist, is a non-sedating anxiolytic in preclinical species but causes sedation in humans. *J. Psychopharmacol. (London, U. K.)* **2011**, 25 (3), 314-328.

23. Atack, J. R.; Wong, D. F.; Fryer, T. D.; Ryan, C.; Sanabria, S.; Zhou, Y.; Dannals, R. F.; Eng, W.-s.; Gibson, R. E.; Burns, H. D.; Vega, J. M.; Vessy, L.; Scott-Stevens, P.; Beech, J. S.; Baron, J.-C.; Sohal, B.; Schrag, M. L.; Aigbirhio, F. I.; McKernan, R. M.; Hargreaves, R. J., Benzodiazepine binding site occupancy by the novel GABAA receptor subtype-selective drug 7-(1,1-dimethylethyl)-6-(2-ethyl-2H-1,2,4-triazol-3-ylmethoxy)-3-(2-fluorophenyl)-1,2,4-triazolo[4,3-b]pyridazine (TPA023) in rats, primates, and humans. *J. Pharmacol. Exp. Ther.* **2010**, 332 (1), 17-25.

24. Ator, N. A.; Attack, J. R.; Hargreaves, R. J.; Burns, H. D.; Dawson, G. R., Reducing abuse liability of GABAA/benzodiazepine ligands via selective partial agonist efficacy at $\alpha 1$ and $\alpha 2/3$ subtypes. *J. Pharmacol. Exp. Ther.* **2010**, 332 (1), 4-16.

25. Russell, M. G. N.; Carling, R. W.; Street, L. J.; Hallett, D. J.; Goodacre, S.; Mezzogori, E.; Reader, M.; Cook, S. M.; Bromidge, F. A.; Newman, R.; Smith, A. J.; Wafford, K. A.; Marshall, G. R.; Reynolds, D. S.; Dias, R.; Ferris, P.; Stanley, J.; Lincoln, R.; Tye, S. J.; Sheppard, W. F. A.; Sohal, B.; Pike, A.; Dominguez, M.; Attack, J. R.; Castro, J. L., Discovery of imidazo[1,2-b][1,2,4]triazines as GABAA $\alpha 2/3$ subtype selective agonists for the treatment of anxiety. *J. Med. Chem.* **2006**, 49 (4), 1235-1238.

26. Van Laere, K.; Bormans, G.; Sanabria-Bohorquez, S. M.; de Groot, T.; Dupont, P.; De Lepeleire, I.; de Hoon, J.; Mortelmans, L.; Hargreaves, R. J.; Attack, J. R.; Burns, H. D., In vivo characterization and dynamic receptor occupancy imaging of TPA023B, an $\alpha 2/\alpha 3/\alpha 5$ subtype selective γ -aminobutyric acid-A partial agonist. *Biol. Psychiatry* **2008**, 64 (2), 153-161.

27. de Haas, S. L.; de Visser, S. J.; van der Post, J. P.; Schoemaker, R. C.; van Dyck, K.; Murphy, M. G.; de Smet, M.; Vessey, L. K.; Ramakrishnan, R.; Xue, L.; Cohen, A. F.; van Gerven, J. M., Pharmacodynamic and pharmacokinetic effects of

MK-0343, a GABA(A) $\alpha_2,3$ subtype selective agonist, compared to lorazepam and placebo in healthy male volunteers. *J Psychopharmacol* **2008**, 22 (1), 24-32.

28. de Haas, S. L.; de Visser, S. J.; van der Post, J. P.; de Smet, M.; Schoemaker, R. C.; Rijnbeek, B.; Cohen, A. F.; Vega, J. M.; Agrawal, N. G.; Goel, T. V.; Simpson, R. C.; Pearson, L. K.; Li, S.; Hesney, M.; Murphy, M. G.; van Gerven, J. M., Pharmacodynamic and pharmacokinetic effects of TPA023, a GABA(A) $\alpha_2,3$ subtype-selective agonist, compared to lorazepam and placebo in healthy volunteers. *J Psychopharmacol* **2007**, 21 (4), 374-383.

29. Atack, J. R.; Hallett, D. J.; Tye, S.; Wafford, K. A.; Ryan, C.; Sanabria-Bohorquez, S. M.; Eng, W. S.; Gibson, R. E.; Burns, H. D.; Dawson, G. R.; Carling, R. W.; Street, L. J.; Pike, A.; De Lepeleire, I.; Van Laere, K.; Bormans, G.; de Hoon, J. N.; Van Hecken, A.; McKernan, R. M.; Murphy, M. G.; Hargreaves, R. J., Preclinical and clinical pharmacology of TPA023B, a GABAA receptor α_2/α_3 subtype-selective partial agonist. *J Psychopharmacol* **2011**, 25 (3), 329-344.

30. Atack, J. R., Subtype-Selective GABA(A) Receptor modulation yields a novel pharmacological profile: The design and development of TPA023. *Adv Pharmacol* **2009**, 57, 137-185.

31. Chen, X.; Jacobs, G.; de Kam, M.; Jaeger, J.; Lappalainen, J.; Maruff, P.; Smith, M. A.; Cross, A. J.; Cohen, A.; van Gerven, J., The central nervous system effects of the partial GABA-A α 2,3 -selective receptor modulator AZD7325 in comparison with lorazepam in healthy males. *Br J Clin Pharmacol* **2014**, 78 (6), 1298-1314.

32. Zuiker, R. G.; Chen, X.; Osterberg, O.; Mirza, N. R.; Muglia, P.; de Kam, M.; Klaassen, E. S.; van Gerven, J. M., NS11821, a partial subtype-selective GABAA agonist, elicits selective effects on the central nervous system in randomized controlled trial with healthy subjects. *J Psychopharmacol* **2016**, 30 (3), 253-262.

33. Omoto, K.; Owen, R. M.; Pryde, D. C.; Watson, C. A. L.; Takeuchi, M. Preparation of Imidazopyridazine Derivatives as GABAA Receptor Modulators. WO2014091368A1, 2014.

34. Owen, R. M.; Pryde, D. C.; Dack, K. N. Preparation of 4-(biphen-3-yl)-1H-pyrazolo[3,4-c]pyridazine Derivatives as GABA Receptor Modulators for Treatment of Epilepsy and Pain. WO2017098367A1, 2017.

35. Owen, R. M.; Pryde, D. C.; Takeuchi, M.; Watson, C. A. L. Preparation of Imidazopyridazine Derivatives as Modulators of the GABAA Receptor Activity. WO2015189744A1, 2015.

36. Nickolls, S. A.; Gurrell, R.; van Amerongen, G.; Kammonen, J.; Cao, L.; Brown, A. R.; Stead, C.; Mead, A.; Watson, C.; Hsu, C.; Owen, R. M.; Pike, A.; Fish, R. L.; Chen, L.; Qiu, R.; Morris, E. D.; Feng, G.; Whitlock, M.; Gorman, D.; van Gerven, J.; Reynolds, D. S.; Dua, P.; Butt, R. P., Pharmacology in translation: the preclinical and early clinical profile of the novel $\alpha 2/3$ functionally selective GABAA receptor positive allosteric modulator PF-06372865. *Br J Pharmacol* **2018**, 175 (4), 708-725.

37. Di, L.; Whitney-Pickett, C.; Umland, J. P.; Zhang, H.; Zhang, X.; Gebhard, D. F.; Lai, Y.; Federico, J. J., 3rd; Davidson, R. E.; Smith, R.; Reyner, E. L.; Lee, C.; Feng, B.; Rotter, C.; Varma, M. V.; Kempshall, S.; Fenner, K.; El-Kattan, A. F.; Liston, T. E.; Troutman, M. D., Development of a new permeability assay using low-efflux MDCKII cells. *J Pharm Sci* **2011**, 100 (11), 4974-4985.

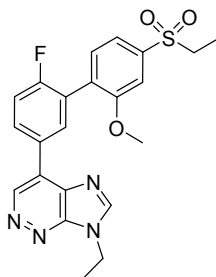
38. Pfeifer, A. M.; Cole, K. E.; Smoot, D. T.; Weston, A.; Groopman, J. D.; Shields, P. G.; Vignaud, J. M.; Juillerat, M.; Lipsky, M. M.; Trump, B. F.; et al., Simian virus 40 large tumor antigen-immortalized normal human liver epithelial cells express hepatocyte characteristics and metabolize chemical carcinogens. *Proc Natl Acad Sci U S A* **1993**, 90 (11), 5123-5127.

39. Kelley, J. L.; Thompson, J. B.; Styles, V. L.; Soroko, F. E.; Cooper, B. R., Synthesis and anticonvulsant of 3H-imidazo[4,5-c]pyridazine, 1H-imidazo[4,5-d]pyridazine and 1H-benzimidazole analog of 9-(2-fluorobenzyl)-6-methylamino-9H-purine. *J. Heterocycl. Chem.* **1995**, 32 (5), 1423-1428.

40. Colacot, T. J.; Shea, H. A., Cp₂Fe(PR₂)₂PdCl₂ (R = i-Pr, t-Bu) complexes as air-stable catalysts for challenging Suzuki coupling reactions. *Org Lett* **2004**, 6 (21), 3731-3734.

41. Sandtorv, A. H.; Bjorsvik, H.-R., Fast halogenation of some N-heterocycles by means of N,N'-dihalo-5,5-dimethylhydantoin. *Adv. Synth. Catal.* **2013**, 355 (2-3), 499-507.

42. Rosini, G.; Ballini, R.; Marotta, E., Functionalized nitroalkanes in synthesis of 1,6-dioxaspiro[4.5]decane components of *Paravespula vulgaris* pheromone. *Tetrahedron* **1989**, 45 (18), 5935-5942.



PF-06372865 (**34**)

The design, optimization and evaluation of a series of novel imidazopyridazine-based subtype-selective positive allosteric modulators (PAMs) for the GABA_A ligand-gated ion channel are described. These efforts ultimately led to the identification of the clinical candidate PF-06372865 (34).